Fisheries and Oceans Canada | Pêches et Océans Canada
Ecosystems and Oceans Science | Sciences des écosystèmes et des océans

Canadian Science Advisory Secretariat (CSAS)

Research Document 2019/055

Newfoundland and Labrador Region

Optical, Chemical, and Biological Oceanographic Conditions on the Newfoundland and Labrador Shelf during 2016-2017

G. Maillet, D. Bélanger, G. Doyle, A. Robar, S. Fraser, J. Higdon, D. Ramsay, P. Pepin

Science Branch
Fisheries and Oceans Canada
PO Box 5667
St. John's, Newfoundland, Canada A1C 5X1

September 2019

Canada

Foreword

This series documents the scientific basis for the evaluation of aquatic resources and ecosystems in Canada. As such, it addresses the issues of the day in the time frames required and the documents it contains are not intended as definitive statements on the subjects addressed but rather as progress reports on ongoing investigations.

Published by:

Fisheries and Oceans Canada
Canadian Science Advisory Secretariat
200 Kent Street
Ottawa ON K1A 0E6

http://www.dfo-mpo.gc.ca/csas-sccs/
csas-sccs@dfo-mpo.gc.ca

© Her Majesty the Queen in Right of Canada, 2019
ISSN 1919-5044

Correct citation for this publication:

Maillet, G., Bélanger, D., Doyle, G., Robar, A., Fraser, S., Higdon, J., Ramsay, D. and P. Pepin. 2019. Optical, Chemical, and Biological oceanographic conditions on the Newfoundland and Labrador Shelf during 2016-2017. DFO Can. Sci. Advis. Sec. Res. Doc. 2019/055.viii + 35 p.

Aussi disponible en français :

Maillet, G., Bélanger, D., Doyle, G., Robar, A., Fraser, S., Higdon, J., Ramsay, D. et P. Pepin. 2019. Conditions optiques, chimiques et biologiques de l'océan sur le plateau de Terre-Neuve-et-Labrador au cours de 2016-2017. Secr. can. de consult. sci. du MPO, Doc. de rech. 2019/055. ix + 40 p.

TABLE OF CONTENTS

TABLE OF TABLES IV
TABLE OF FIGURES IV
ABSTRACT VIII
INTRODUCTION 1
METHODS 2
SAMPLE COLLECTION 2
OPTICAL PROPERTIES 4
VERTICALLY INTEGRATED VARIABLES 4
SATELLITE REMOTE-SENSING OF OCEAN COLOUR 4
OBSERVATIONS 7
OPTICAL AND BIOLOGICAL PROPERTIES – HIGH FREQUENCY SAMPLING STATION 7
NUTRIENTS AND PHYTOPLANKTON – HIGH FREQUENCY SAMPLING STATION AND OCEANOGRAPHIC SECTIONS 8
Remote-sensing of ocean colour 14
ZOOPLANKTON 19
High frequency sampling station 19
Zooplankton abundance and biomass 19
Copepod abundance 20
Copepod phenology 21
Oceanographic sections 22
Zooplankton biomass 22
Zooplankton abundance 23
Calanus finmarchicus 24
Pseudocalanus spp. 25
Oithona spp. 26
Non-copepod zooplankton 27
Spatial distribution 29
DISCUSSION 33
SUMMARY 34
ACKNOWLEDGMENTS 35
REFERENCES 35

TABLE OF TABLES

Table 1. Atlantic Zone Monitoring Program (AZMP) sampling missions in Newfoundland and Labrador Region in 2016 and 2017. Hydro stations are the total sum of CTD profiles conducted during respective missions including both partial stations (CTD only) and complete occupations including CTD profile, water sampling and net tows. 3

TABLE OF FIGURES

Figure 1. Map showing spring, summer, and fall AZMP section occupations along with surface ocean chlorophyll a conditions during 2016 and 2017 1

Figure 2. Statistical sub-regions in the Northwest Atlantic identified for spatial/temporal analysis of Satellite Ocean Colour data. 6

Figure 3. Optical and chlorophyll a pigment properties determined from in-situ PAR (photosynthetic active radiation) and combination of discrete extracted and fluorometric (calibrated) chlorophyll a profiling at high frequency monitoring station (S27) during 1999 to 2017..... 7

Figure 4. Comparison of vertical structure of silicate (top panels) and nitrate (middle panels) in mmol m^{-3} and chlorophyll concentrations (lower panels) in mg m^{-3} with mean conditions from 1999-2015 (left panels) with 2016 (middle panels) and 2017 (right panels) at the NL region high frequency sampling coastal station. Gridding method to generate contour plots using triangulation with linear interpolation. Missing monthly observations in 2016-2017 are shown in black. 9

Figure 5. Comparison of annual variability in nutrient inventories (silicate and nitrate) in 2016-2017 with mean conditions from 1999-2015 at the Newfoundland and Labrador Region fixed station (S27). The vertical lines are the standard error of the monthly means. 10

Figure 6. Comparison of annual variability in chlorophyll a inventories in 2016-2017 with mean conditions from 1999-2015 at the Newfoundland and Labrador Region fixed station (S27). The vertical lines are the standard error of the monthly means. 11

Figure 7. Time series of shallow (0-50 m) silicate and nitrate (combined nitrite and nitrate) inventory anomalies from different oceanographic sections and high frequency sampling station S27 during 1999-2017. The contribution from each of the sections and fixed station is represented by colour and height of the vertical bar. The solid black line is the cumulative (composite) anomaly across all sites in a given year.....12

Figure 8. Time series of deep (50m-150 m) silicate and nitrate (combined nitrite and nitrate) inventory anomalies from different oceanographic sections and high frequency sampling station during 1999-2017. The contribution from each of the sections and fixed station is represented by colour and height of the vertical bar. The solid black line is the cumulative (composite) anomaly across all sites in a given year. 13

Figure 9. Time series of chlorophyll a anomalies from different oceanographic sections and high frequency sampling station during 1999-2017. The contribution from each of the sections and fixed station is represented by colour and height of the vertical bar. The solid black line is the cumulative (composite) anomaly across all sites in a given year.....14

Figure 10. Biweekly surface chlorophyll a concentrations (mg m^{-3}), from VIIRS ocean colour imagery in the North Atlantic during 2016. Top panels are biweekly composite imagery from April and bottom panels for May. Normal ice-cloud-covered periods are blocked out in white. Imagery obtained from Bedford Institute of Oceanography - Semi-Monthly Composites. 15

Figure 11. Biweekly surface chlorophyll a concentrations (mg m^{-3}), from VIIRS ocean colour imagery in the North Atlantic during 2017. Top panels are biweekly composite imagery from April and bottom panels for May. Normal ice-cloud-covered periods are blocked out in white. Imagery obtained from Bedford Institute of Oceanography - Semi-Monthly Composites. 16

Figure 12. Summary of annual ocean colour anomalies across the different NL statistical sub-regions during 1998 to 2017. The top panel is the integrated biomass while the bottom panel indicates the amplitude (peak intensity) of the spring production cycle derived from the shifted Gaussian model (see methods for description of metrics). 17

Figure 13. Summary of annual ocean colour anomalies across the different NL statistical sub-regions during 1998 to 2017. The timing indices derived from the shifted Gaussian distribution include peak timing (top panel), and duration of the spring bloom (bottom panel). The solid black line is the cumulative (composite) anomaly across all sub-regions in a given year. Negative anomalies for peak timing indicate earlier blooms while positive anomalies indicate the opposite. 18

Figure 14. Total zooplankton abundance (upper left panel), and biomass of combined (upper right panel), small (lower left panel) and large (lower right panel) size fraction of zooplankton at the high-frequency sampling station S27 for the 1999-2015 reference period (grey line) and for the years 2016 (black circle) and 2017 (white circle). Monthly means (SE) for the reference period were calculated using least square means derived from a linear model with the factors Year (1999 to 2015), and Season (spring, summer and fall). 19

Figure 15. Monthly relative abundance of main zooplankton taxonomic groups at Station 27 for the 1999-2015 reference period (left panel), and for the years 2016 (middle panel) and 2017 (right panel). White rectangles in the middle (year 2016) and right (year 2017) panels represent period of the year with no data collection. 20

Figure 16. Total copepod abundance (upper left panel) and abundance of large Calanus finmarchicus (upper right panel), Calanus glacialis (center left panel), Calanus hyperboreus (center right panel) and small Pseudocalanus spp.(lower left panel), Oithona spp. (lower right panel) copepods at the high frequency sampling station S27 for the 1999-2015 reference period (grey line) and for 2016 (black circle) and 2017 (white circle). Monthly means (SE) for the reference period were calculated using least square means derived from a linear model with the factors Year (1999 to 2015), and Season (spring, summer and fall).....21

Figure 17. Intra-annual variation in the relative abundance of copepodite stage I-VI for Calanus finmarchicus (top panels) and Pseudocalanus spp. (bottom panels) for the 1999-2015 reference period, and during the sample years 2016 and 2017. White rectangles in the middle (year 2016) and right (year 2017) panels represent period of the year with no data collection. 22

Figure 18. Annual standardized anomalies of zooplankton biomass on four oceanographic sections [Southeast Grand Bank (SEGB); Flemish Cap (FC); Bonavista Bay (BB); Seal Island (SI)], from 1999 to 2017. Annual anomalies of log transformed biomass [ln (biomass g m^{-2} + 1)] were calculated for each section using least square mean (ls mean) and standard deviation (SD) derived from a linear model with fixed factors Year, Season and Station. Mean log transformed biomass (SD) for the 1999-2015 the reference period were: SEGB = 2.96 (0.93); FC = 4.88 (1.04); BB = 6.97 (2.31); SI = 6.27 (2.63). Anomalies within ±0.5 SD (horizontal dashed lines) of the reference period mean are considered normal. 23

Figure 19. Annual standardized anomalies of zooplankton abundance on four oceanographic sections [Southeast Grand Bank (SEGB); Flemish Cap (FC); Bonavista Bay (BB); Seal Island (SI)] from 1999 to 2017. For each section, annual anomalies of log transformed abundance [ln (individuals m^{-2} + 1)] were calculated using least square means derived from a linear model with

fixed factors Year, Season and Station. Mean log transformed abundances (SD) for the 1999-2015 reference period were: SEGB = 118.36 (10.50); FC = 121.88 (13.48); BB = 135.01 (12.10); SI = 116.65 (15.18). Anomalies within ±0.5 SD (horizontal dashed lines) of the reference period mean are considered normal. 24

Figure 20. Annual standardized anomalies of Calanus finmarchicus abundance on four oceanographic sections [Southeast Grand Bank (SEGB); Flemish Cap (FC); Bonavista Bay (BB); Seal Island (SI)] from 1999 to 2017. Annual anomalies of log transformed abundance [ln (individuals m^{-2} + 1)] were calculated using least square means derived from a linear model with fixed factors Year, Season and Station. Mean log transformed abundances (SD) for the 1999-2015 reference period were: SEGB = 8.04 (0.64); FC = 9.10 (0.34); BB = 9.66 (0.30); SI = 9.54 (0.68). Anomalies within ±0.5 SD (horizontal dashed lines) of the reference period mean are considered normal. 25

Figure 21. Annual standardized anomalies of Pseudocalanus spp. abundance on four oceanographic sections [Southeast Grand Bank (SEGB); Flemish Cap (FC); Bonavista Bay (BB); Seal Island (SI)] from 1999 to 2017. Annual anomalies of log transformed abundance [ln (individuals m^{-2} + 1)] were calculated using least square means derived from a linear model with fixed factors Year, Season and Station. Mean log transformed abundances (SD) for the 1999-2015 reference period were: SEGB = 9.70 (0.42); FC = 8.42 (0.51); BB = 9.06 (0.39); SI = 9.92 (0.69). Anomalies within ±0.5 SD (horizontal dashed lines) of the reference period mean are considered normal. 26

Figure 22. Annual standardized anomalies of Oithona spp. abundance on four oceanographic sections [Southeast Grand Bank (SEGB); Flemish Cap (FC); Bonavista Bay (BB); Seal Island (SI)] from 1999 to 2017. Annual anomalies of log transformed abundance [ln (individuals m^{-2} + 1)] were calculated using least square means derived from a linear model with fixed factors Year, Season and Station. Mean log transformed abundances (SD) for the 1999-2015 reference period were: SEGB = 10.74 (0.31); FC = 10.43 (0.31); BB = 10.25 (0.30); SI = 10.24 (0.77). Anomalies within ±0.5 SD (horizontal dashed lines) of the reference period mean are considered normal. 27

Figure 23. Annual standardized anomalies of non-copepod abundance on four oceanographic sections [Southeast Grand Bank (SEGB); Flemish Cap (FC); Bonavista Bay (BB); Seal Island (SI)] from 1999 to 2017. Annual anomalies of log transformed abundance [ln (individuals m^{-2} + 1)] were calculated using least square means derived from a linear model with fixed factors Year, Season and Station. Mean log transformed abundances (SD) for the 1999-2015 reference period were: SEGB = 35.53 (4.18); FC = 33.54 (6.02); BB = 34.11 (4.77); SI= 31.21 (6.51). Anomalies within ±0.5 SD (horizontal dashed lines) of the reference period mean are considered normal. 28

Figure 24. Annual relative abundance of main non-copepod zooplankton groups on four oceanographic sections [Southeast Grand Bank (SEGB); Flemish Cap (FC); Bonavista Bay (BB) Seal Island (SI)] from 1999 to 2017. 29

Figure 25. Spring zooplankton abundance per station along three oceanographic sections [Bonavista Bay (BB); Flemish Cap (FC); Southeast Grand Bank (SEGB)] for the climatological reference period (left), year 2016 (middle) and 2017 (right). Lighter to darker colour gradient of the ocean represents the 100, 300 and 1000 m isobaths. Black arrow indicates the location of the Avalon Channel (AC). 30

Figure 26. Summer zooplankton abundance per station along three oceanographic sections [Seal Island (SI); Bonavista Bay (BB); Flemish Cap (FC)] for the climatological reference period (left), year 2016 (middle) and 2017 (right). Lighter to darker colour gradient of the ocean

represents the 100, 300 and 1000 m isobaths. Black arrow indicate the location of the Avalon Channel (AC). 31

Figure 27. Autumn zooplankton abundance per station along four oceanographic sections [Seal Island (SI); Bonavista Bay (BB); Flemish Cap (FC); Southeast Grand Bank (SEGB)] for the climatological reference period (left), year 2016 (middle) and 2017 (right). Lighter to darker colour gradient of the ocean represents the 100, 300 and 1000 m isobaths. Black arrow indicate the location of the Avalon Channel (AC).....32

ABSTRACT

The overall pattern of variation among the nutrients and lower trophic levels surveyed in this report (phytoplankton biomass and zooplankton abundance) highlighted the relationship between biogeochemical conditions (nitrate standing stock) and primary (phytoplankton biomass) and secondary (zooplankton abundance and biomass) production.

Optical and chlorophyll *a* indices indicate reduction in phytoplankton biomass and delayed timing of the production cycle at the high frequency sampling station (S27) in 2016 – 2017. The replenishment of key macronutrients in the deep (> 50 m) strata has undergone further reduction in recent years. The absence of an autumn bloom may be related to changes in renewal processes. The deep inventories of macronutrients across the standard oceanographic sections have transitioned from mostly positive to mainly negative anomalies in the last decade. Phytoplankton biomass have declined overall in line with the trends in macronutrient inventories. Increased abundance of zooplankton observed throughout the northwest Atlantic may also contribute to higher grazing pressure and reduction of phytoplankton standing stocks.

The general trend of increasing zooplankton abundance observed over the past nineteen years continued during 2016 – 2017 with abundance reaching historical highs from southern Labrador to the southern Grand Banks. In contrast, the biomass of zooplankton remained below the climatology in all oceanographic sections and was at a record low on the southern Labrador shelf and on the Grand Banks. The abundance of large copepods (*Calanus finmarchicus, Calanus hyperboreus*), which has been declining for 3-5 years throughout much of the region, remained low on the Newfoundland and Labrador (NL) Shelf but showed signs of recovery on the Grand Banks. The abundance of small copepods (*Pseudocalanus spp., Oithona similis, Microcalanus spp., Oncea spp.*) and other non-copepod organisms continued to increase throughout the region. The production cycle of early copepodite stages of keystone copepods species (*Calanus finmarchicus* and *Pseudocalanus spp.*) was delayed by ~1 month in 2016 and 2017 compared to climatology at S27, possibly because of the delayed spring bloom and general cooling and freshening of the system in that area. More research is needed to understand the mechanisms behind the observed shift in zooplankton community structure and their potential impacts at higher trophic levels.

INTRODUCTION

The Atlantic Zone Monitoring Program (AZMP) was implemented in 1998 with the aim of increasing Fisheries and Oceans Canada's (DFO) capacity to understand, describe, and forecast the state of the marine ecosystem and to quantify the changes in the ocean physical, chemical and biological properties. A critical element of the AZMP involves an observation program aimed at assessing the variability in nutrients, phytoplankton (microscopic plants) and zooplankton (drifting animals). The overall aim is to identify fundamental relationships among elements of the planktonic ecosystem and establish how they respond to changes in environmental drivers.

The AZMP derives its information on the state of the marine ecosystem from data collected at a network of sampling locations (high frequency sampling stations, cross-shelf sections, and groundfish surveys) in each region (Quebec, Gulf, Maritimes, Newfoundland and Labrador) sampled at a frequency of every two weeks to once annually. The location of the standard sections for the Newfoundland and Labrador (NL) region occupied in 2016 and 2017 is shown in Figure 1.

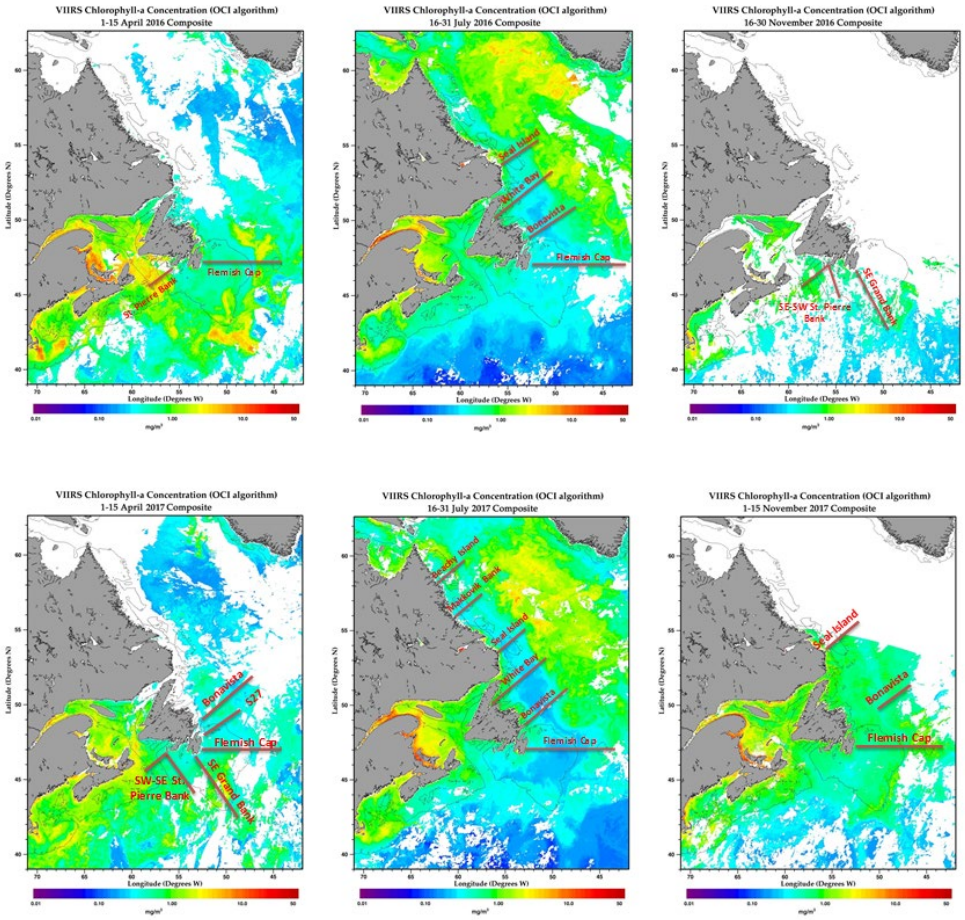

Figure 1. Map showing spring, summer, and fall AZMP section occupations along with surface ocean chlorophyll a conditions during 2016 (upper panels) and 2017 (lower panels). The 2016 spring/fall and 2017 fall AZMP missions were impacted by availability of vessels. White areas on maps indicate extensive cloud and/or ice coverage.

A description of the seasonal patterns in the distribution of phytoplankton and zooplankton provides important information about organisms that form the base of the marine foodweb. An understanding of the production cycles of plankton, and their interannual variability, is an essential part of an ecosystem approach to fisheries management. This report provides an assessment of the distribution and abundance of macronutrients and plankton on the NL Shelves highlighting the biological oceanographic conditions in 2016-17 in relation to long-term average conditions based on archived data. It complements similar reviews of the biological oceanographic conditions in the Gulf of St. Lawrence and the Scotian Shelf and Gulf of Maine as part of the Atlantic Zone Monitoring Program (Johnson et al. 2018; Blais et al. 2018). When possible, the long-term averages were standardized to a climatological average from 1999 to 2015 and compared with individual years to compute annual anomalies. This report also complements ocean climate and physical oceanographic assessments of the Region (e.g. Cyr et al. 2019) and for the Northwest Atlantic shelf system as a whole (DFO 2018).

Variability in biological oceanographic conditions may be driven by physical properties of the water column. Typically, the water masses characteristic of the NL Shelf are dominated by subpolar waters with a sub-surface temperature range typically below 0°C. Labrador slope water flows southward along the shelf edge and into the Flemish Pass; this water mass is generally warmer and saltier than the subpolar shelf waters. On average, bottom temperatures remain <0°C over most of the northern Grand Bank but increase to > 0°C in southern regions and at depths below 200 m along the slopes of the banks. North of the Grand Bank, bottom temperatures are generally warmer except for the shallow inshore regions where they are mainly <0°C. Throughout most of the year the cold, relatively fresh water overlying the shelf is separated from the warmer higher-density water of the continental slope region by a strong temperature and density front. This winter-formed water mass is generally referred to as the Cold Intermediate Layer (CIL) and is considered a reliable index of ocean climate conditions. In general, shelf water masses undergo seasonal modification in their properties as a result of the seasonal cycles of air-sea heat flux, wind-forced mixing and ice formation and melt, leading to intense vertical and horizontal gradients particularly along the frontal boundaries separating the shelf and slope water masses.

METHODS

To the extent possible, sample collection and processing conforms to established standard protocols (Mitchell et al. 2002). Non-standard measurements or derived variables are described below.

SAMPLE COLLECTION

Three seasonal (spring, summer, fall) surveys were conducted along standard (primary sections include; Seal Island, Bonavista, Flemish Cap, and Southeast Grand Banks) oceanographic sections in the NL region during the 2016 and 2017 calendar years, in addition to occupations of the high frequency sampling coastal station (Station 27 [S27]) during ecosystem trawl surveys (Table 1, Figure 1).

Table 1. *Atlantic Zone Monitoring Program (AZMP) sampling missions in Newfoundland and Labrador Region in 2016 and 2017. Hydro stations are the total sum of conductivity, temperature, depth (CTD) profiles conducted during respective missions including both partial stations (CTD only) and complete occupations including CTD profile, water sampling and net tows.*

Group	Location	Mission ID	Dates	# Hydro Stations	# Net / Bottle Stations
Ecosystem Trawl Surveys	NE Newfoundland Shelf and Grand Bank	TEL2016-159-172	May 10-Jun 21, 2016	540	6 / 5
-	Grand Bank, NE Newfoundland and Labrador Shelf	NED2016-464-472, TEL2016-162-167	Aug 21-Dec 20, 2016	658	17 / 9
-	-	NED476-482	Mar 31-Jun 22, 2017	435	10/4
-	-	TEL178-183	Oct 5-Dec 20, 2017	731	6/4
Seasonal Sections	St. Pierre Bank	TEL2016-157	Apr 1-6, 2016	7	7
-	Grand Bank	TEL2016-159	May 11-17, 2016	26	26
-	-	TEL2017-173	Apr 6-23, 2017	129	76
S27	Grand Bank and NE Newfoundland and Labrador Shelf	TEL2016-160	July 8-28, 2016	137	69
	-	TEL2017-176	July 8-28, 2017	174	80
	NE Newfoundland and Labrador Shelf and Grand Bank	DIS009-015	Nov 11-19, Dec 9 - 16, 2017	106	44
	Avalon Channel	Ships of Opportunity	Apr 16-Dec 16, 2016	45	19/12
	-	-	Apr 6-Dec 20, 2017	31	16/8

A total of 1413 and 1606 hydrographic stations were occupied in 2016 and 2017, respectively. Plankton and seawater sampling were collected at a total of 272 and 248 stations in 2016 and 2017, respectively. The high frequency sampling S27 station was sampled 45 and 35 times during April through December in 2016 and 2017, but no occupations were possible in the winter months. Oceanographic sample collections for S27 and standard sections include a conductivity, temperature, depth (CTD) high resolution profile using a Sea-Bird Electronics SBE-9plus instrument equipped with dissolved oxygen, chlorophyll *a* (chl*a*) fluorescence, photosynthetic active radiation (PAR), pH, Coloured Dissolved Organic Matter (CDOM) and transmissometer sensors. Niskin water bottle samples were collected using a CTD-rosette at standard depths of 5, 10, 20, 30, 40, 50, 75, 100, 150 m, and near bottom for calibration of salinity and oxygen, chl*a* and nutrient analyses. In addition to the standard discrete water sampling program for biological and chemical conditions, particulate organic carbon and nitrogen, as well as carbonate (total alkalinity and total dissolved inorganic carbon) are routinely collected at a subset of stations and depths but are not reported here. Zooplankton samples were collected using dual vertical ring net plankton assemblies from a maximum depth of

1000 m using a dual-202 µm or 202-70 µm for taxonomic, abundance, and biomass analyses of zooplankton.

OPTICAL PROPERTIES

The vertical attenuation coefficient (K_d) was derived from in-water light extinction measurements using a CTD-rosette mounted PAR meter. The downward vertical attenuation coefficient of PAR ($K_{d\text{-}PAR}$) was estimated from the linear regression of $\ln(E_d(z))$ versus depth z (where $E_d(z)$ is the value of downward PAR irradiance at z m) in the depth interval from near surface to 50 m. When in-water PAR data were not available, the vertical attenuation coefficient was calculated by:

K_d_chl*a* (m^{-1}) = 0.027 m^{-1} + 0.015 m^{-1} + B(z) * 0.04 m^{-1} (Platt et al. 1988)

where B(z) is the concentration of chl*a* in mg m^{-3}. We substituted calibrated chl*a* from *in-situ* chl*a* fluorescence when discrete data were not available at depth z meters. The additional coefficients in this equation are related to the components of pure seawater and dissolved substances. The average value of K_d was calculated for the upper water column using the chl*a* profile in the upper 50 m. The estimate of euphotic depth (ca. depth of 1 % incident PAR) was computed from:

Z_{eu} (m) = 4.6 / $K_{d\text{-}PAR}$

We substituted K_d_chl*a* when $K_{d\text{-}PAR}$ was not available to compute the euphotic depth.

VERTICALLY INTEGRATED VARIABLES

Annual estimates of water column inventories (using trapezoidal numerical integration) of nutrients (0-50 m and 50-150 m), chl*a* (0-100 m), the mean abundance of key zooplankton taxa at both the fixed site and as an overall average along each of the four standard sections were based on general linear models (GLMs) of the form:

$$Ln(Density) = \alpha + \beta_{YEAR} + \delta_{MONTH} + \varepsilon$$

for S27, where *Density* is in units of m^{-2}, α is the intercept, β and δ are categorical effects for year and month effects, and ε is the error, and

$$Ln(Density) = \alpha + \beta_{YEAR} + \delta_{STATION} + \gamma_{SEASON} + \varepsilon$$

to derive an estimate of the interannual variations based on all occupations of the sections, where δ takes into account the effect of station location and γ takes into account variation among seasons. Density was log-transformed to deal with the skewed distribution of the observations. In the case of zooplankton, one was added to the *Density* term to include observations where no animals of a given taxa were counted in the sample. Average integrated optical and nutrient and chl*a* inventories were not transformed. An estimate of the least squares means based on type III sums of squares was used as the measure of the overall year effect (β). Because the model estimates are adjusted annually as a result of the input of new data, *YEAR* effects tend to vary from one assessment to the next but any changes are verified against the raw data to ensure that the underlying spatial (*STATION*) or temporal (*SEASON*) patterns along each section are maintained. Large departures from previous patterns could be indicative of shifts in the dominant regime or ecosystem processes.

SATELLITE REMOTE-SENSING OF OCEAN COLOUR

Satellite observations provide a comprehensive spatial and temporal view of surface phytoplankton biomass. Phytoplankton biomass was estimated from ocean colour data collected

by the Sea-viewing Wide Field-of-view Sensor (SeaWiFS) ; Moderate Resolution Imaging Spectroradiometer (MODIS) "Aqua" sensor, and the Visible-Infrared Imager Radiometer Suite (VIIRS) sensor. The SeaWiFS time series began in the September of 1997, MODIS data stream began in July, 2002, and VIIRS availability is January 2012 to present. Composite images of 8-days for chl*a* for the entire NW Atlantic (39-62.5° N Latitude 42-71° W Longitude) were routinely produced from SeaWiFS/MODIS/VIIRS data[1]. Basic statistics (mean, range, standard deviation, etc.) were extracted from the composites for selected statistical sub-regions as shown in Figure 2. Satellite data do not provide information on the vertical structure of chl*a* in the water column but do provide highly resolved (~1.5 km) data on their geographical distribution in surface waters at the large scale.

We constructed an ocean colour time series from 1998 to 2017 using data from the available satellite sensors using the following periods; 1998-2007 SeaWiFS, 2008-2011 MODIS, and 2012-2016 VIIRS. We used the shifted Gaussian function of time model to describe the characteristics of the seasonal cycle of phytoplankton production (Zhai et al. 2011). Four different metrics were computed using satellite composite data during the spring bloom to characterize the integral (magnitude) of chl*a* concentration under the Gaussian curve (mg m^{-2} d^{-1}), peak intensity of the spring bloom (mg m^{-3}), the peak-timing of the spring bloom peak (Julian day), and duration of the spring bloom cycle (days).

[1] Bedford Institute of Oceanography - Operational Remote Sensing

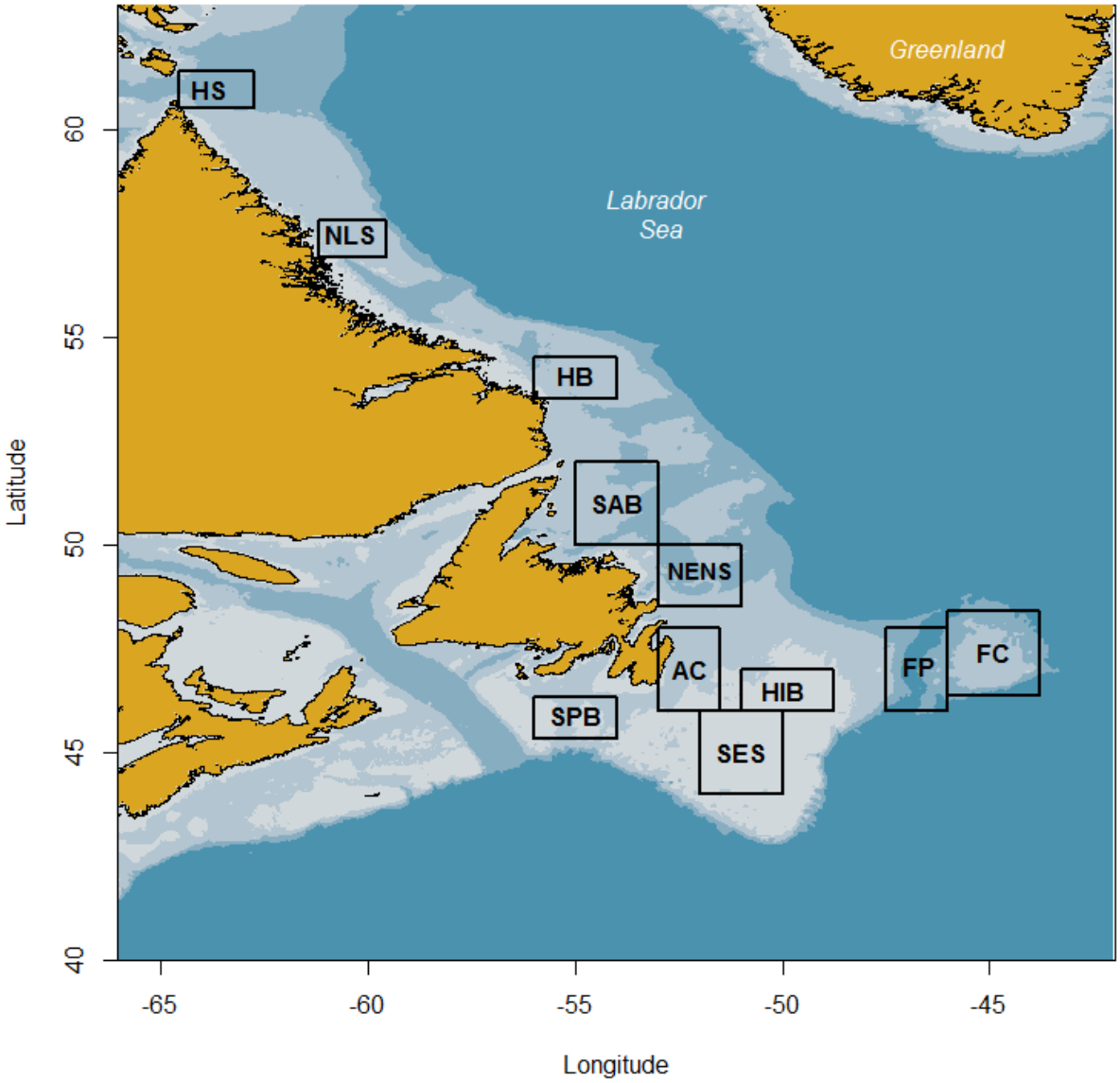

Figure 2. *Statistical sub-regions in the Northwest Atlantic identified for spatial/temporal analysis of Satellite Ocean Colour data. Sub-regions in the Newfoundland and Labrador region include St. Pierre Bank (SPB), Southeast Shoal (SES), Avalon Channel (AC), Hibernia (HIB), Flemish Pass (FP) and Flemish Cap (FC), Northeast Newfoundland Shelf (NENS), St. Anthony Basin (SAB), Hamilton Bank (HB), Northern Labrador Shelf (NLS), and Hudson Strait (HS).*

OBSERVATIONS

OPTICAL AND BIOLOGICAL PROPERTIES – HIGH FREQUENCY SAMPLING STATION

Optical indices generally track the dynamics of the phytoplankton production cycle. Attenuation of photosynthetic active radiation (PAR) gradually increases over the winter with a peak in April followed by a rapid decline through June (Figure 3). Thereafter, the index remains relatively stable throughout the summer and fall. The observed values in 2016-2017 were generally lower in April indicating limited spring blooms and a delay of 1 month in 2017 compared to the climatology. The index was higher in 2017 compared to 2016 and the climatology throughout the summer and fall periods. The euphotic depth describing the penetration of PAR to 1 % levels generally varies between 60 to 85 m throughout the year except during the spring bloom where values show substantial reduction to as low as 15 m. Observations in 2016 were generally deeper than the climatology while the reverse was true in 2017 which were generally more shallow than the corresponding reference period. The optical measurements closely match the pattern observed in integrated (0-100 m) chl*a* index based on extracted pigment and calibrated fluorescence. Short-term episodic summer and autumn blooms observed by the optical sensors coincide with the observed temporal changes in chl*a* biomass compared with background levels during winter and late fall. The inventory of chla during the spring bloom consistently lower throughout 2016-2017 compared to the climatology. Observations during the summer and fall indicated biomass was lower in 2016 compared to 2017 which was near or slightly above the reference period.

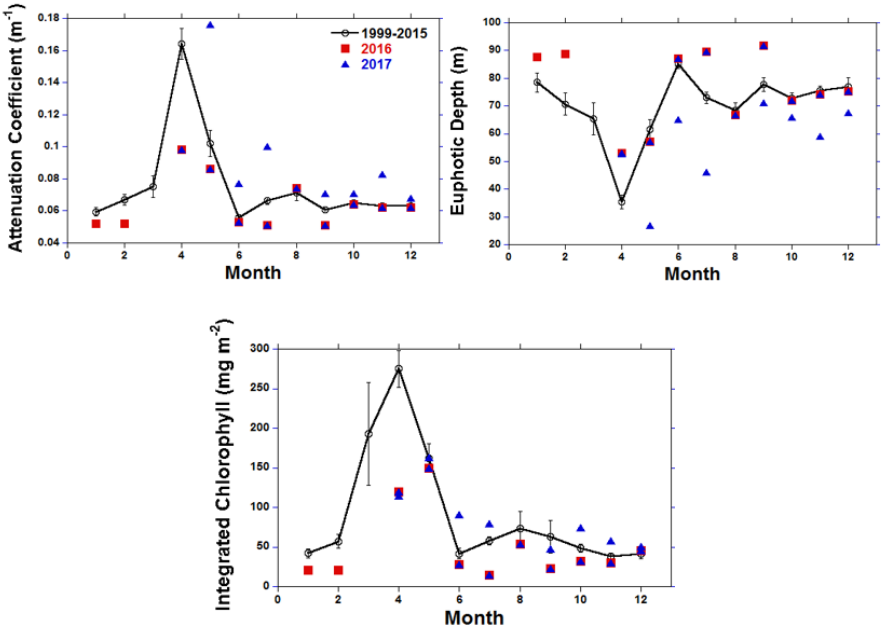

Figure 3. *Optical and chlorophyll a pigment properties determined from in-situ PAR (photosynthetic active radiation) and combination of discrete extracted and fluorometric (calibrated) chlorophyll a profiling at high frequency monitoring station (S27) during 1999 to 2017. The solid black line is the monthly mean climatology during 1999-2015 with standard errors. Vertical attenuation coefficient (top left panel; data only from 2000 onward) for the upper 50 m of the water column determined from PAR or model estimate derived from calibrated in-situ chlorophyll a fluorescence, euphotic zone depth based on PAR and/or derived from in-situ chlorophyll a or calibrated fluorescence (right top panel), and integrated chlorophyll a within the upper 100 m of the water column based on extracted pigment (bottom panel).*

NUTRIENTS AND PHYTOPLANKTON – HIGH FREQUENCY SAMPLING STATION AND OCEANOGRAPHIC SECTIONS

The vertical distributions of inorganic nutrients (nitrate, silicate, and phosphate) included in the observational program of the AZMP show strong seasonal co-variation. For this reason, and because the availability of nitrogen and silicate is most often associated with limiting the growth of phytoplankton, more emphasis in this report was placed on variability in these nutrient inventories. The inventories of nutrients are influenced by seasonal biological processes operating throughout the upper water-column. In addition, determining the initiation of nutrient uptake is dependent on sampling effort, and frequency of observations is limited in winter and early spring compared to other times of the year.

Dominant features of the annual production cycle were inferred from comparison of climatological vertical structure and monthly variability in the concentration of nutrients and chlorophyll during the reference period (1999-2015). Rapid changes in near-surface silicate and nitrate from > 4-5 mmol m^{-3} during winter to < 1 mmol m^{-3} by early April coincide with the onset of the spring phytoplankton bloom, which is followed by a renewal of surface concentrations in late autumn (Figure 4). The climatology reveals the extent of the uptake in silicate and nitrate is rapid beginning in late March extending to depths of 50 m and gradually deepening through to autumn. The timing of uptake in macronutrient concentrations in 2016 was similar to the reference period but delayed by 2 months in 2017 (Figure 4). The vertical extent of the drawdown in silicate was more extensive in 2017 compared to the previous year and the climatology. In addition, there was limited renewal of both silicate and nitrate in 2017 with the delayed uptake that extended into the late autumn. The vertical extent of chlorophyll *a* biomass during the reference period shows concentrations reaching near 4 mg m^{-3} during the spring bloom in the upper 50 m with the production cycle extending from March through the end of May (Figure 4). Phytoplankton biomass declines rapidly to background levels during early summer with a limited autumn bloom that varies from late August through early October. Chlorophyll *a* biomass observed in 2016 and 2017 was 2-fold lower in biomass during the spring bloom, and there was a delay in the onset of the production cycle in 2017. However, limited sampling in 2017 partially obscures spring bloom initiation. It is also possible that the sampling program may have missed a portion of the production cycle since the uptake of macronutrients was comparable to the reference period in 2016 and 2017.

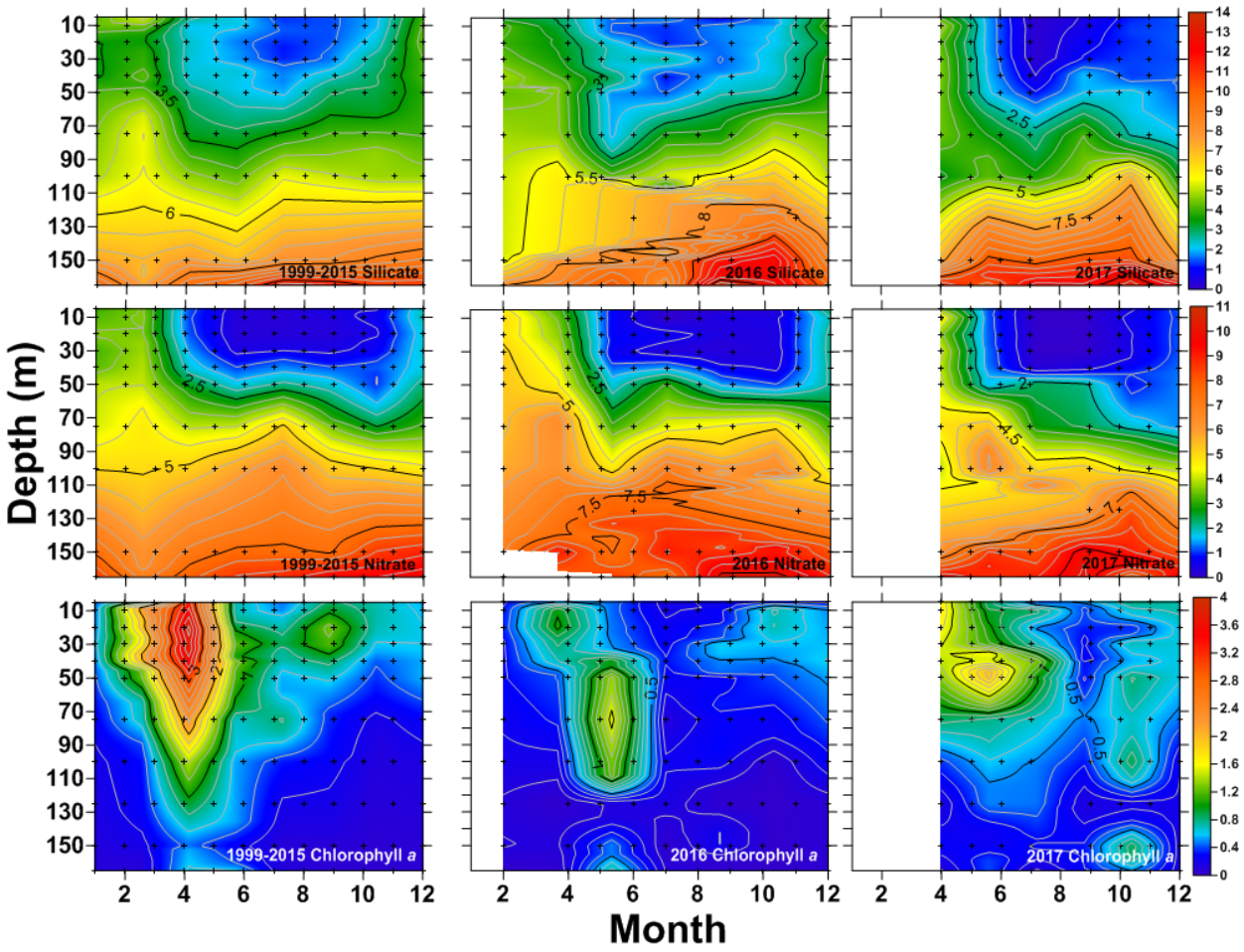

Figure 4. *Comparison of vertical structure of silicate (top panels) and nitrate (middle panels) in mmol m^{-3} and chlorophyll concentrations (lower panels) in mg m^{-3} with mean conditions from 1999-2015 (left panels) with 2016 (middle panels) and 2017 (right panels) at the NL region high frequency sampling coastal station. Gridding method to generate contour plots using triangulation with linear interpolation. Missing monthly observations in 2016-2017 are shown in black.*

A summary of monthly inventories of macronutrients from S27 during the standard reference period and 2016-2017 reveal the rapid uptake in the upper 50 m in contrast to deeper layers that show more limited change (Figure 5). The average monthly trends indicate peak inventories of silicate and nitrate in the shallow (< 50 m) layer in February followed by a rapid depletion beginning in March with minima by May-June. The observations clearly show the delay in uptake during the spring bloom during 2016-2017 compared to the reference period although no monthly data were available from January through March during recent years (Figure 5). After the spring bloom, renewal of silicate inventories is relatively rapid reaching high levels by late autumn in contrast to nitrate, which remains low throughout the upper water column in summer and autumn. The processes of renewal of macronutrients within the upper water column were comparable in 2016-2017 with the reference period. Deep inventories (> 50 m) of silicate were well below normal in June-July 2016-2017 while nitrate was depleted in May and December months compared to the seasonal climatology (Figure 5).

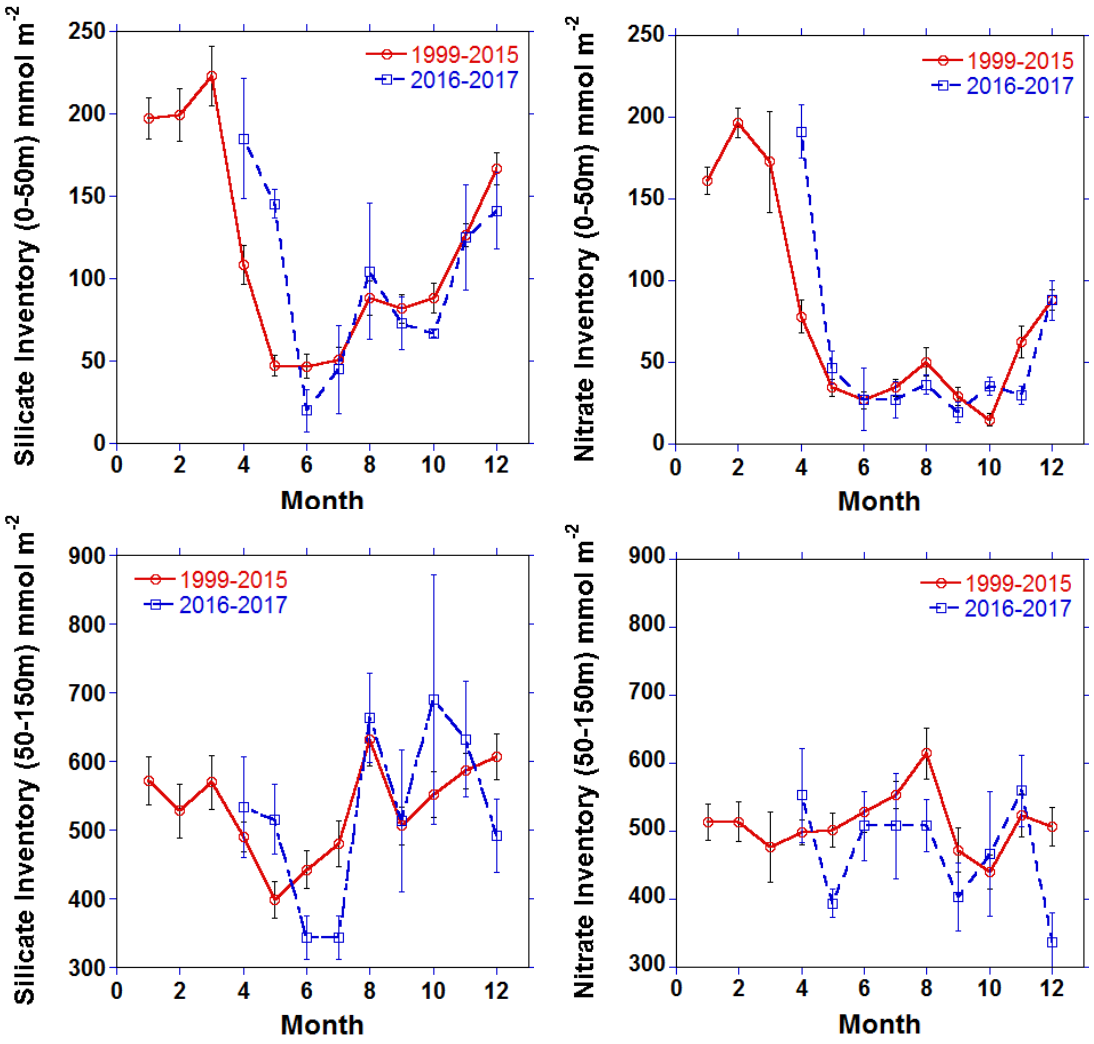

Figure 5. *Comparison of annual variability in nutrient inventories (silicate and nitrate) in 2016-2017 with mean conditions from 1999-2015 at the Newfoundland and Labrador Region fixed station (S27). The vertical lines are the standard error of the monthly means.*

The delay in uptake detected in both macronutrients in 2016-2017 coincided with a weaker and delayed (~ 1 month) spring bloom compared to the reference period (Figure 6). The chlorophyll *a* inventories in the upper 100 m normally exceed > 250 mg m^{-2} but, only reached 150 mg m^{-2} in 2016-2017. The absence of an autumn bloom was also apparent in recent years compared to the standard climatology.

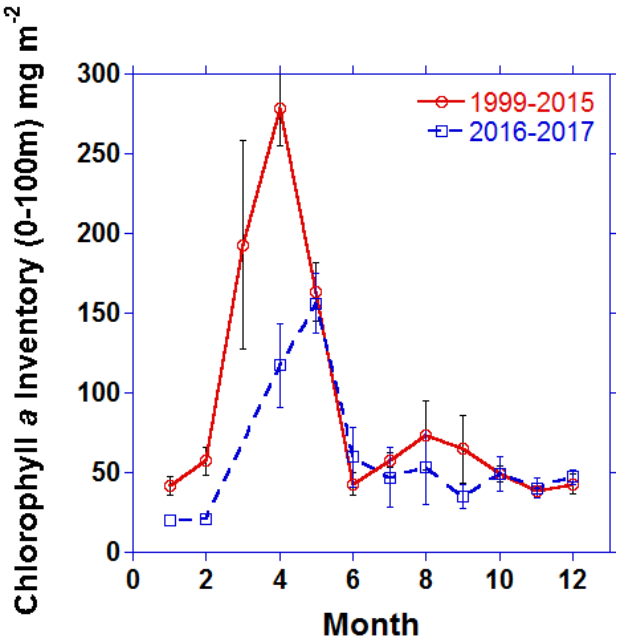

Figure 6. *Comparison of annual variability in chlorophyll a inventories in 2016-2017 with mean conditions from 1999-2015 at the Newfoundland and Labrador Region fixed station (S27). The vertical lines are the standard error of the monthly means.*

Time series of seasonally-adjusted annual anomalies of nutrient availability along the different standard sections and S27 were used to assess long-term trends. In general, the macronutrient inventories show some short-term coherent trends along with high variability between positive and negative annual anomalies during the 19-year time series (Figure 7). Shallow silicate inventories varied between positive and negative anomalies with a record-low/high cumulative anomaly in 2012 and 2003 respectively with a general negative trend over the series. Silicate inventories in the upper water-column have returned to near normal levels in 2016-2017 since the record-low observed in 2012. The inventories of nitrate in the shallow layer also show a downward trend from the early 2000's until 2013 but have since recovered to above normal levels in 2017 (Figure 7).

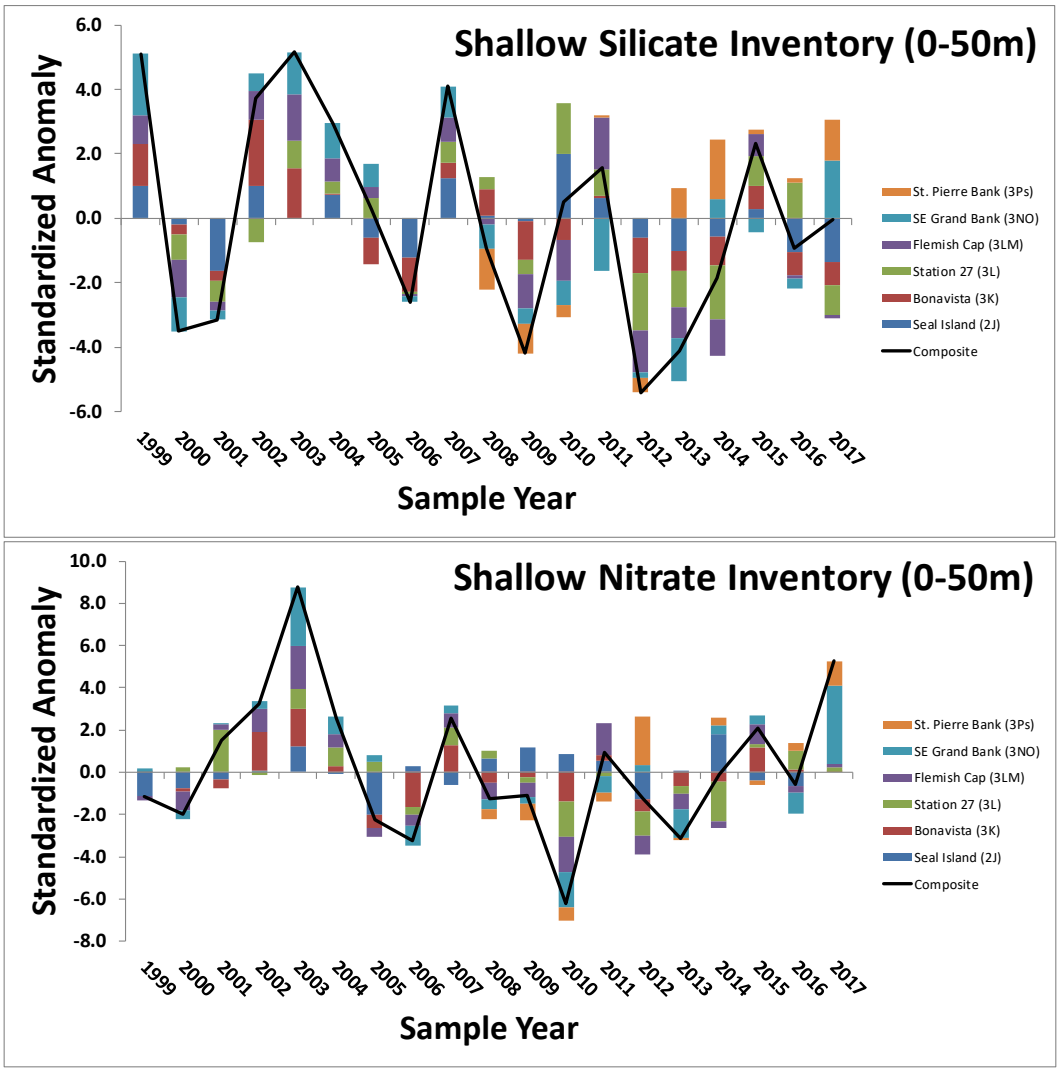

Figure 7. *Time series of shallow (0-50 m) silicate and nitrate (combined nitrite and nitrate) inventory anomalies from different oceanographic sections and high frequency sampling station S27 during 1999-2017. The contribution from each of the sections and fixed station is represented by colour and height of the vertical bar. The solid black line is the cumulative (composite) anomaly across all sites in a given year.*

The time series of deep inventories for silicate and nitrate show a transition from mostly positive anomalies in the first half of the series followed by mainly negative anomalies in the latter period (Figure 8). The decline in silicate inventories began near the start of the series while nitrate began to decline after 2007. In 2016-2017, deep inventories of macronutrients has returned to near normal over the large cumulative negative anomalies observed across the sections and S27 during 2012-2015.

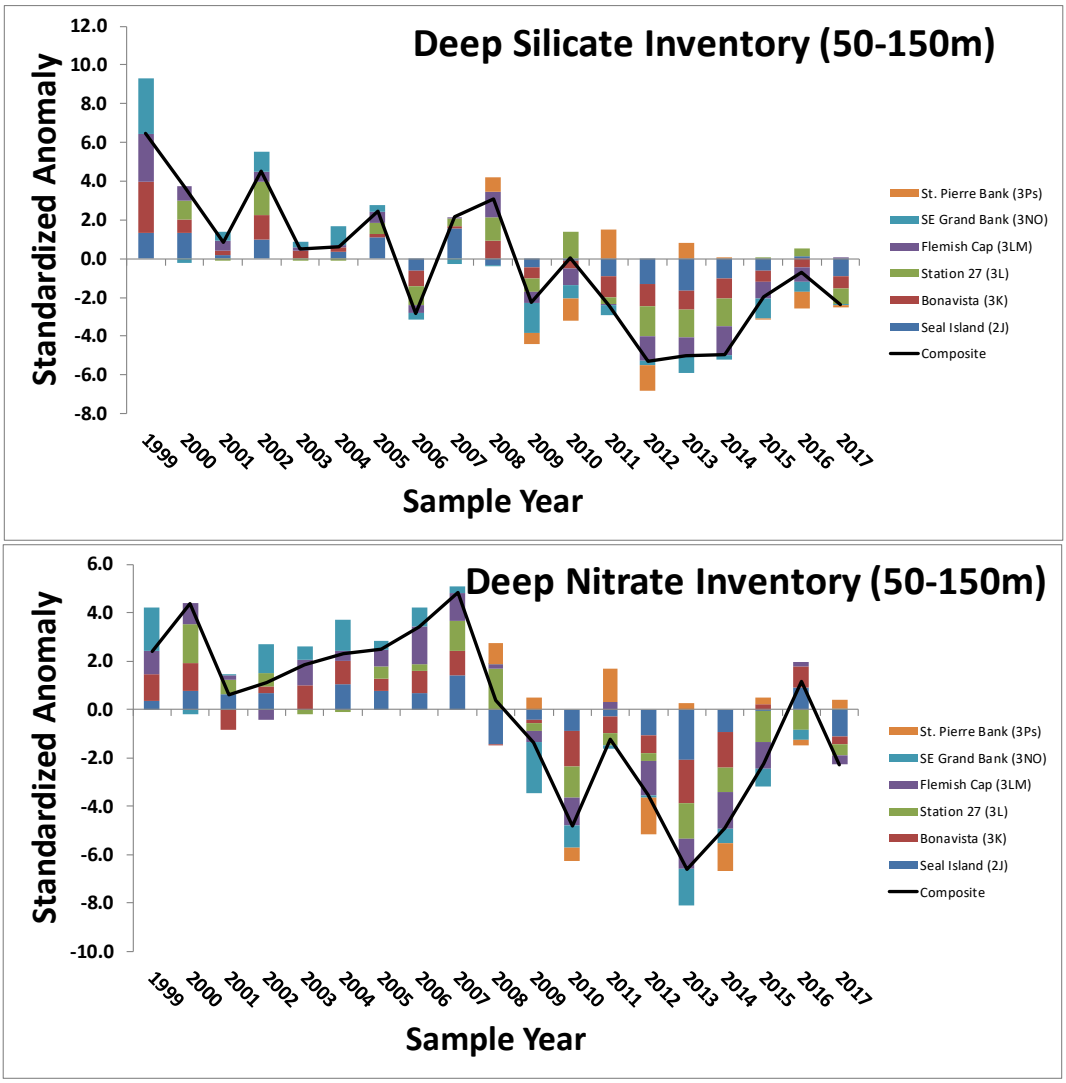

Figure 8. *Time series of deep (50m-150 m) silicate and nitrate (combined nitrite and nitrate) inventory anomalies from different oceanographic sections and high frequency sampling station during 1999-2017. The contribution from each of the sections and fixed station is represented by colour and height of the vertical bar. The solid black line is the cumulative (composite) anomaly across all sites in a given year.*

Phytoplankton biomass inferred from chlorophyll a inventories across the standard sections and S27 have declined overall in line with the general pattern in deep macronutrient levels (Figure 9). One would expect some lag between these indices given the time required to mix water from depth into the upper mixed layer to fuel new primary production. There is some indication of improvement in phytoplankton biomass in recent years with an increasing trend since 2015. Annual anomalies remain mostly negative since 2011, reaching a record-low in 2015. Although the cause for the observed transition to lower macronutrient concentrations in deep water is unclear, the lower levels in macronutrient inventories may in part contribute to the observed changes in timing and intensity of the spring bloom throughout the NL region.

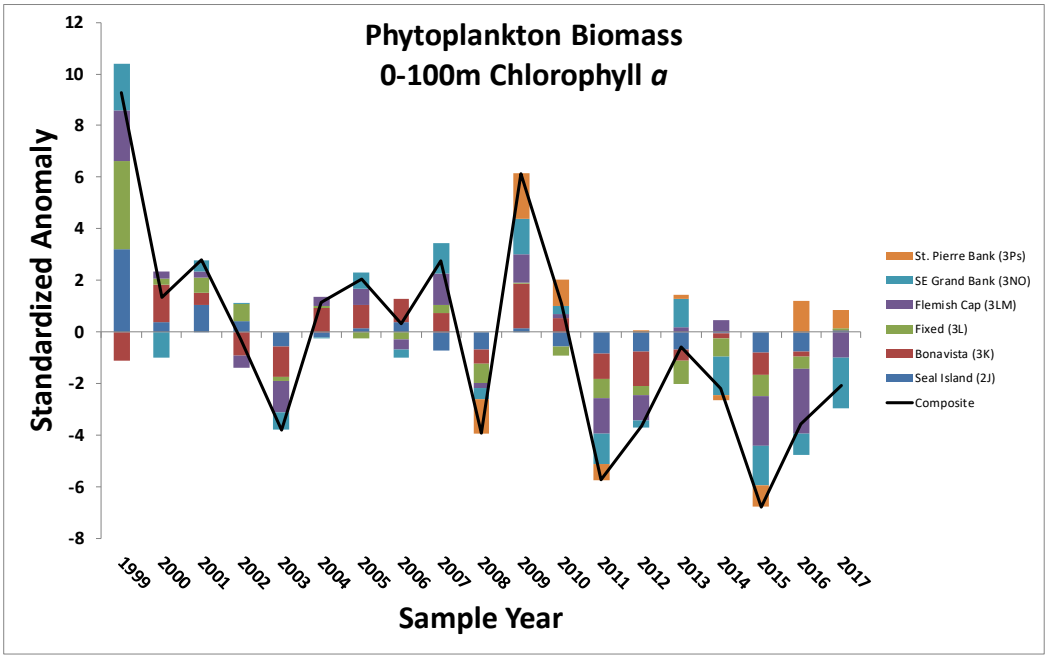

Figure 9. *Time series of chlorophyll a anomalies from different oceanographic sections and high frequency sampling station during 1999-2017. The contribution from each of the sections and fixed station is represented by colour and height of the vertical bar. The solid black line is the cumulative (composite) anomaly across all sites in a given year.*

Remote-sensing of ocean colour

Satellite ocean colour (VIIRS) data provides a large-scale perspective of surface phytoplankton biomass (chl*a*) over the whole of the NW Atlantic that is not possible for conventional vessel-based sampling. Using satellite composite images of sub-regions supplements our ship-based observations and provides seasonal coverage and a large-scale context with which to interpret our survey data. The ocean colour imagery provides information about the timing and spatial extent of the spring and autumn blooms but does not provide information of the dynamics that take place below the top few meters of the water column. Subsurface information is achieved using the high frequency sampling at S27 and the broad scale oceanographic surveys.

Observations of ocean colour over the North Atlantic reveal associated changes in the timing and intensity of the spring bloom in 2016-2017 as detected by VIIRS ocean colour imagery. The early development of enhanced surface blooms started in early April in 2016 on the tail of the Grand Bank and southern Shelf waters (Figure 10). The spring bloom gradually intensified over the eastern half of the Grand Bank along the Shelf-Slope frontal areas and continued to propagate to the northeast Newfoundland Shelf by early May, with chl*a* concentrations well above background levels (~ 1 mg m^{-3}). By late May surface chla concentrations throughout the Grand Bank had returned back to background levels. In 2017, the initiation of the spring bloom was slightly later in April over the Grand Bank but, more intense and covered a larger area compared to 2016 (Figure 11). Much of the surface activity of the spring production was largely confined to the southern portion of the Grand Bank with minimal activity observed northwards along the northeast Shelf. Surface chl*a* levels begin to transition back to background levels by late May in 2017 similar to conditions observed in 2016. Significant ice and cloud coverage do not permit an evaluation of surface activity further north on the Labrador Shelf. Elevated surface concentrations of chl*a* are observed in the Labrador Sea, particularly in 2016 with large scale

blooms beginning in the south in late May and propagating northwards through early June (not shown).

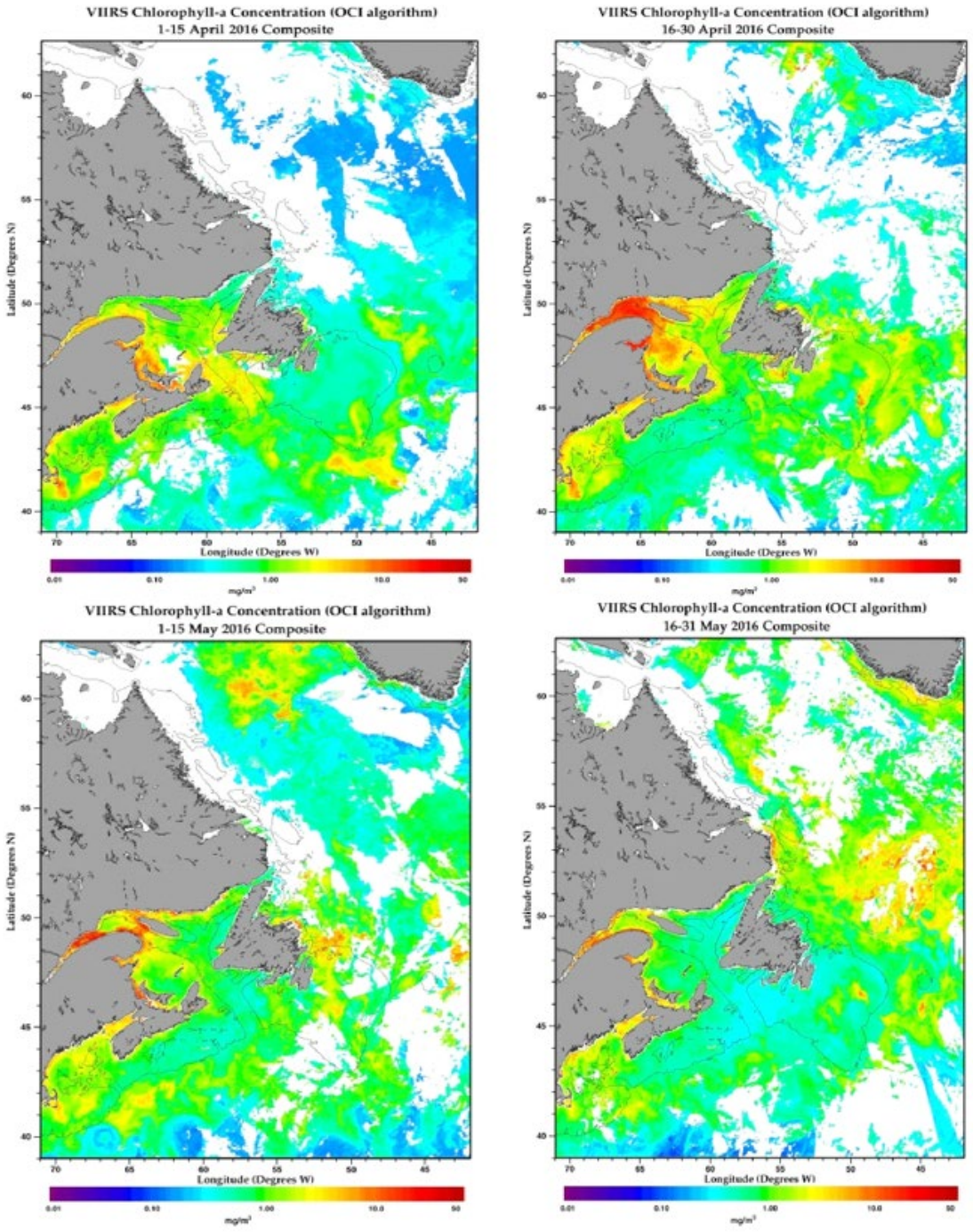

Figure 10. *Biweekly surface chlorophyll a concentrations (mg m^{-3}), from VIIRS ocean colour imagery in the North Atlantic during 2016. Top panels are biweekly composite imagery from April and bottom panels for May. Normal ice-cloud-covered periods are blocked out in white. Imagery obtained from* Bedford Institute of Oceanography - Semi-Monthly Composites.

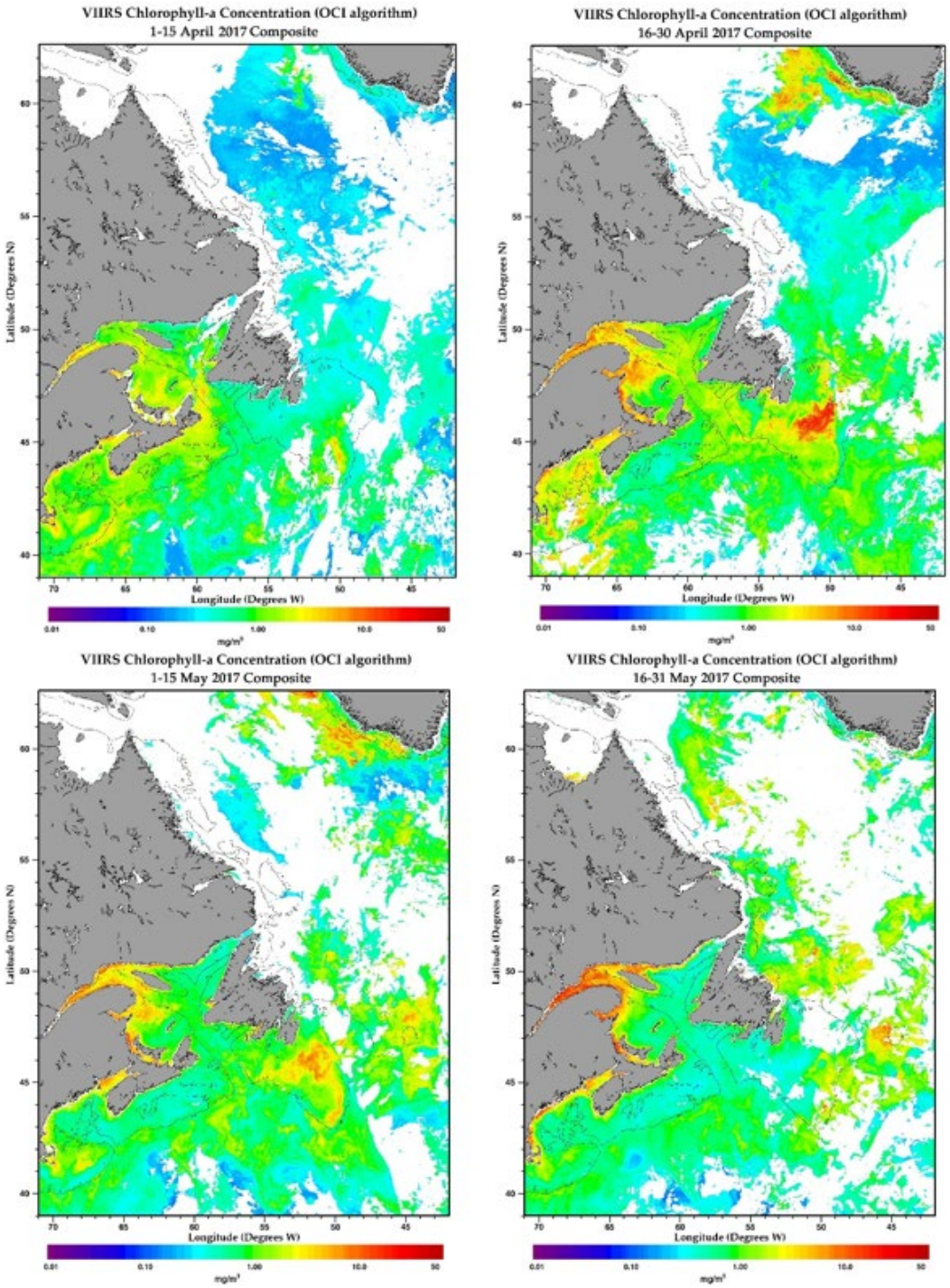

Figure 11. *Biweekly surface chlorophyll a concentrations (mg m^{-3}), from VIIRS ocean colour imagery in the North Atlantic during 2017. Top panels are biweekly composite imagery from April and bottom panels for May. Normal ice-cloud-covered periods are blocked out in white. Imagery obtained from* Bedford Institute of Oceanography - Semi-Monthly Composites.

Data was insufficient in some of the northern areas to permit parameter estimation of the different metrics in certain years. Overall, the magnitude (integrated chl*a* biomass) and

amplitude (peak intensity) of the spring bloom was below normal across most of the NL sub-regions in 2016 (record-low) and 2017 compared to the standard reference period (1998-2015). The downward trend in the magnitude and amplitude indices began after the record peak value observed in 2011 with most sub-regions shifting to negative anomalies thereafter (Figure 12).

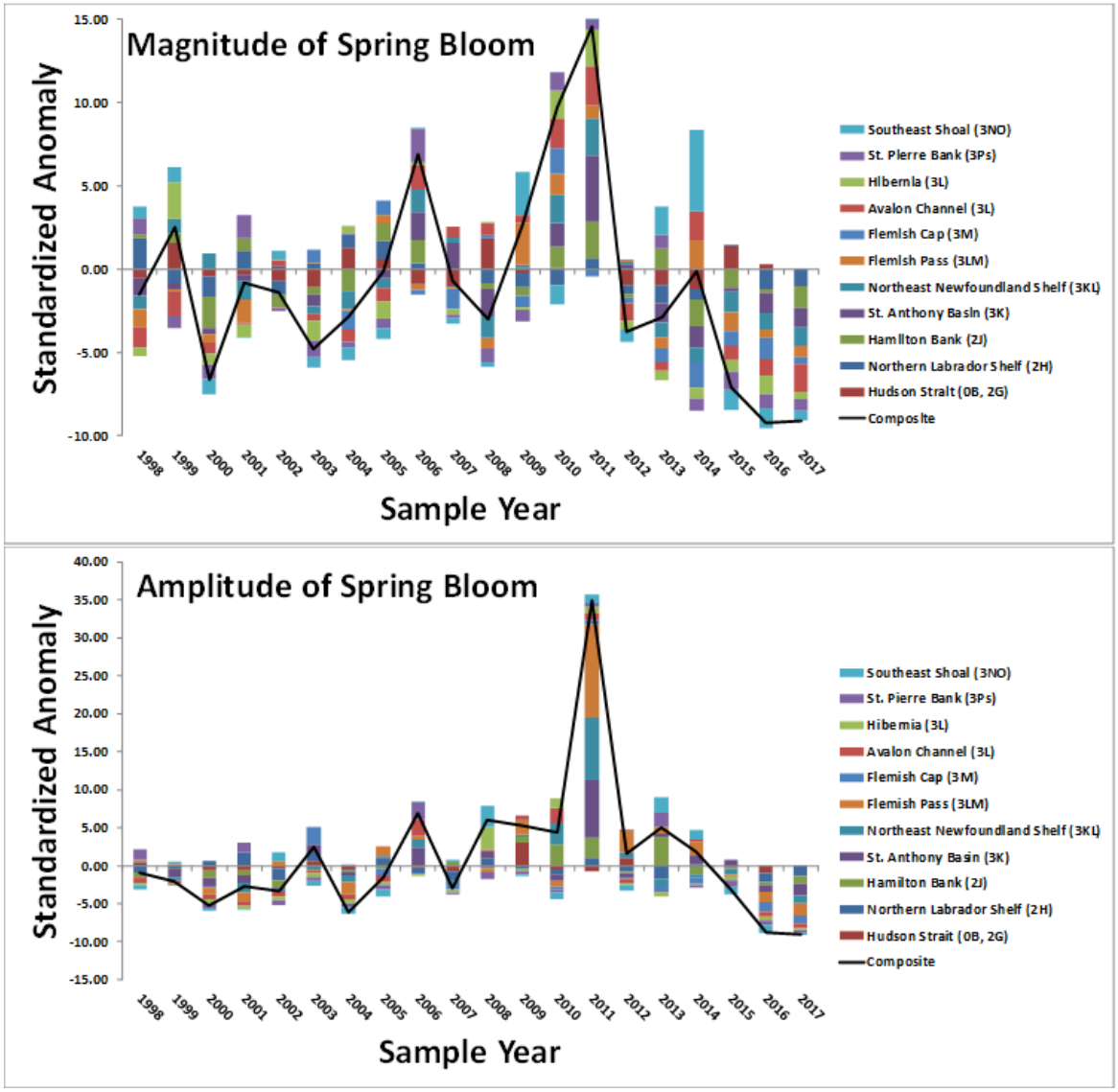

Figure 12. *Summary of annual ocean colour anomalies across the different NL statistical sub-regions during 1998 to 2017. The top panel is the integrated biomass while the bottom panel indicates the amplitude (peak intensity) of the spring production cycle derived from the shifted Gaussian model (see methods for description of metrics).*

The peak time of the spring bloom transitioned between periods of early versus late blooms throughout the 20-year time series based on the cumulative composite index (Figure 13). Delayed blooms occurred in the early 2000's and mid-2010's along with recent years. Early blooms were apparent during 2005-2006 along with the record early bloom observed in 2010. The anomalies have stayed above normal (late blooms) for peak timing since 2013 (Figure 13). Although the timing of the bloom has transitioned between early and late periods, the duration of the spring bloom has gradually declined from the late 1990's to 2015 based on the composite

index. Bloom duration shifted back to above normal in 2016-2017 after a period of sustained negative anomalies observed during 2011 to 2015.

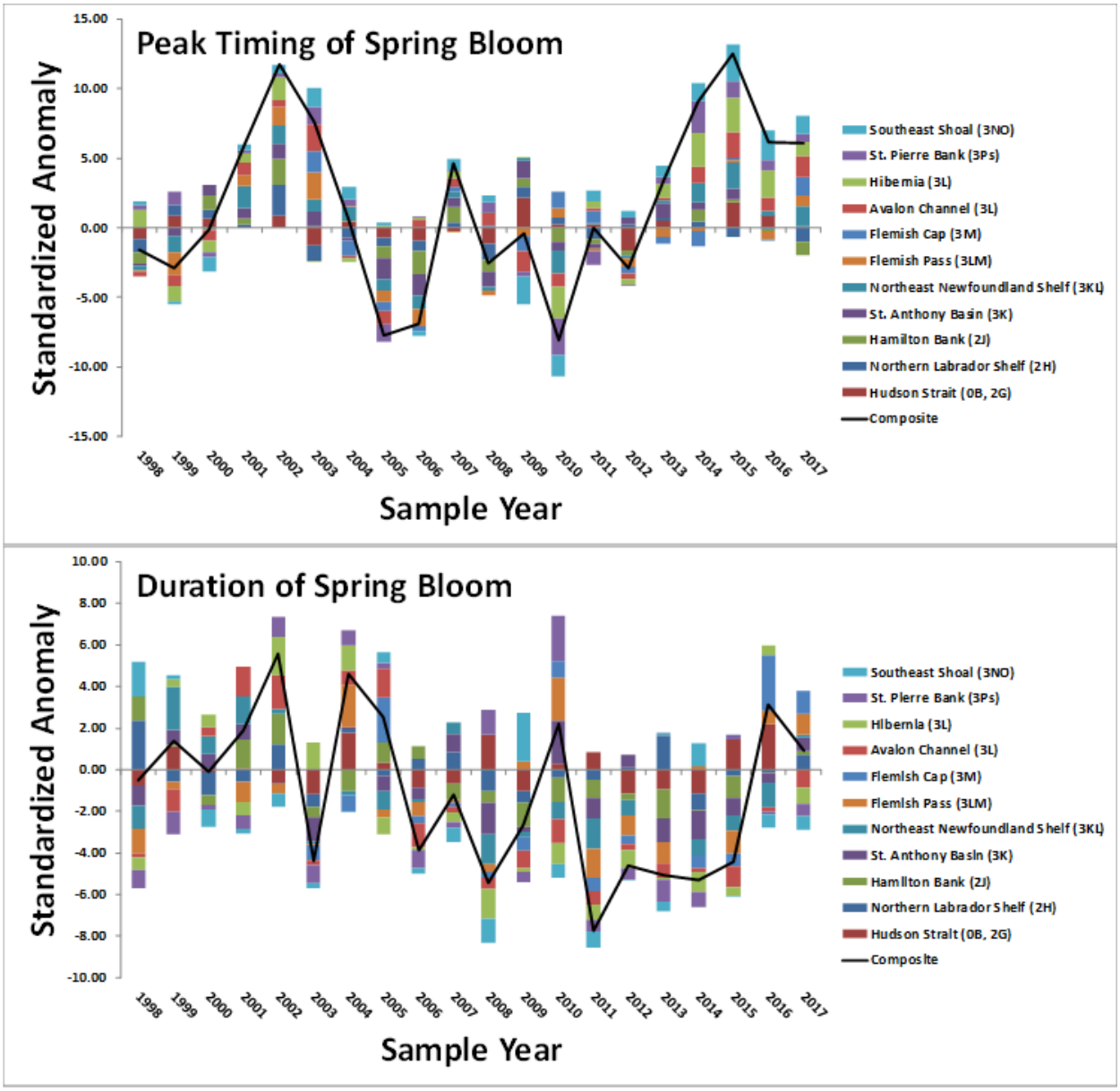

Figure 13. *Summary of annual ocean colour anomalies across the different NL statistical sub-regions during 1998 to 2017. The timing indices derived from the shifted Gaussian distribution include peak timing (top panel), and duration of the spring bloom (bottom panel). The solid black line is the cumulative (composite) anomaly across all sub-regions in a given year. Negative anomalies for peak timing indicate earlier blooms while positive anomalies indicate the opposite.*

ZOOPLANKTON

High frequency sampling station

Zooplankton abundance and biomass

At S27, total zooplankton abundance is typically highest in January and declines throughout winter and spring to a minimum in May. Abundance increases again during summer and stays relatively high during the rest of the year (July - December). In 2016, zooplankton abundance remained mostly near or above climatology and was especially high in autumn (August – November). In 2017, abundance was mostly near or below climatology during spring and summer (April to June) but above normal in autumn (October to December). Autumn abundances were more than double the climatology in ~30% and ~50% of the samples collected in 2016 and 2017, respectively. Total zooplankton biomass is typically lowest in January, increases over the winter and early spring to a maximum of ~5 g m^{-2} in April. Biomass then gradually declines until August and levels at ~2 g m^{-2} until December when it starts to decline again. The biomass of small (< 1 mm) zooplankton is highest during winter and early spring (January - April) whereas the biomass of large (> 1 mm) zooplankton is highest during the spring (April – June). The biomass of smaller zooplankton remained mostly below climatology throughout 2016 and 2017. The biomass of large zooplankton was mostly below normal in 2016, especially from April to July with values ~2.5 times lower than climatology. Biomass of large zooplankton was generally higher in 2017 than in 2016 and remained near or above climatology during June and July (Figure 14).

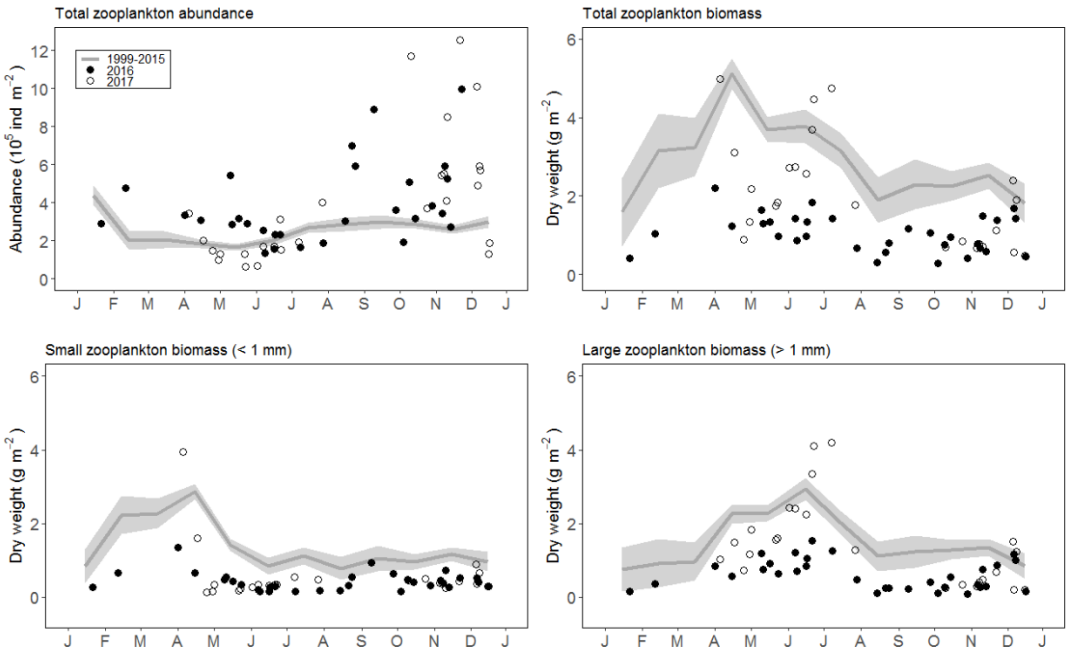

Figure 14. *Total zooplankton abundance (upper left panel), and biomass of combined (upper right panel), small (lower left panel) and large (lower right panel) size fraction of zooplankton at the high-frequency sampling station S27 for the 1999-2015 reference period (grey line) and for the years 2016 (black circle) and 2017 (white circle). Monthly means (SE) for the reference period were calculated using least square means derived from a linear model with the factors Year (1999 to 2015), and Season (spring, summer and fall).*

Typically, copepods account for 89% of total zooplankton abundance at S27, followed by tunicates (5%), mollusks (4%) and other non-copepod crustaceans (<1%). The relative abundance of tunicates (mostly *Oikopleura* and *Frittilaria* spp.) peaks in May and remains high throughout the summer while the proportion of mollusks is highest during autumn. Non-copepod Crustaceans (mostly cladocerans and euphausiids) are present from July-October with maximum relative abundance observed in August. In 2016 and 2017, the proportion of tunicates in the water column was higher than the climatology, peaking at ~21% in both years compared to 10% for the long-term mean. In 2016, mollusk relative abundance was lower than climatology during summer and autumn whereas annual crustaceans distribution was similar to the climatology. Characterization of zooplankton relative distribution among taxonomic groups in 2017 was limited by large temporal gaps in sampling during winter and summer (Figure 15).

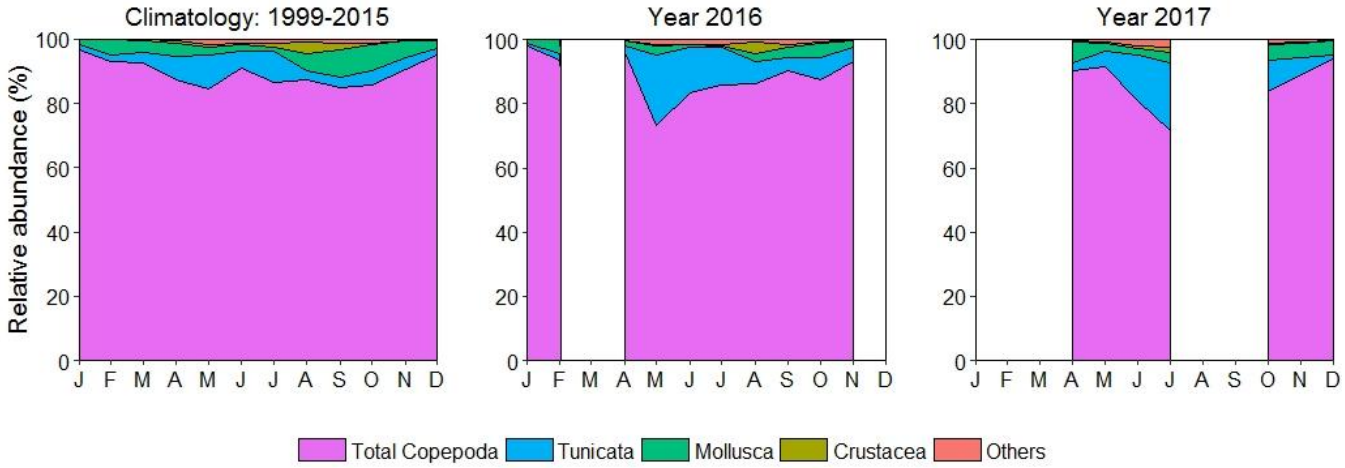

Figure 15. *Monthly relative abundance of main zooplankton taxonomic groups at Station 27 for the 1999-2015 reference period (left panel), and for the years 2016 (middle panel) and 2017 (right panel). White rectangles in the middle (year 2016) and right (year 2017) panels represent period of the year with no data collection.*

Copepod abundance

Total copepod abundance at S27 is typically highest in January, decreases during winter and spring to a minimum in May, and increases through summer to an autumn plateau. Abundance normally starts to increase again in December towards the annual maximum one month later. Abundance of the large temperate-subarctic calanoid copepod *Calanus finmarchicus* is normally characterized by a rapid increase from a minimum in April to maximum in July, followed by a gradual decline throughout autumn and winter. Abundance of more arctic calanoid copepods *C. glacialis* and *C. hyperboreus* normally peaks between May and July and remains low throughout the rest of the year. Although these two species occur in relatively low abundance at S27, they can significantly contribute to overall zooplankton biomass because of their larger body size. Abundance of the small calanoid copepod *Pseudocalanus* spp. is normally low in spring (February – March), peaks in July, and gradually decreases until November when it starts increasing again. Changes in the seasonal abundance of the small cyclopoid copepod *Oithona* spp. at S27 is characterized by very high winter abundances, a spring minimum in May and intermediate autumn values. In 2016 and 2017, total copepod abundance was mostly near or above normal, especially from August to December when abundances often exceeded climatology by several orders of magnitude. Abundance of large calanoid copepods was mostly near or below normal except for the high abundances of *C. hyperboreus* recorded during June and July of 2017, whereas abundance of small copepods was mostly near or above normal with markedly high values recorded between August and December in both years (Figure 16).

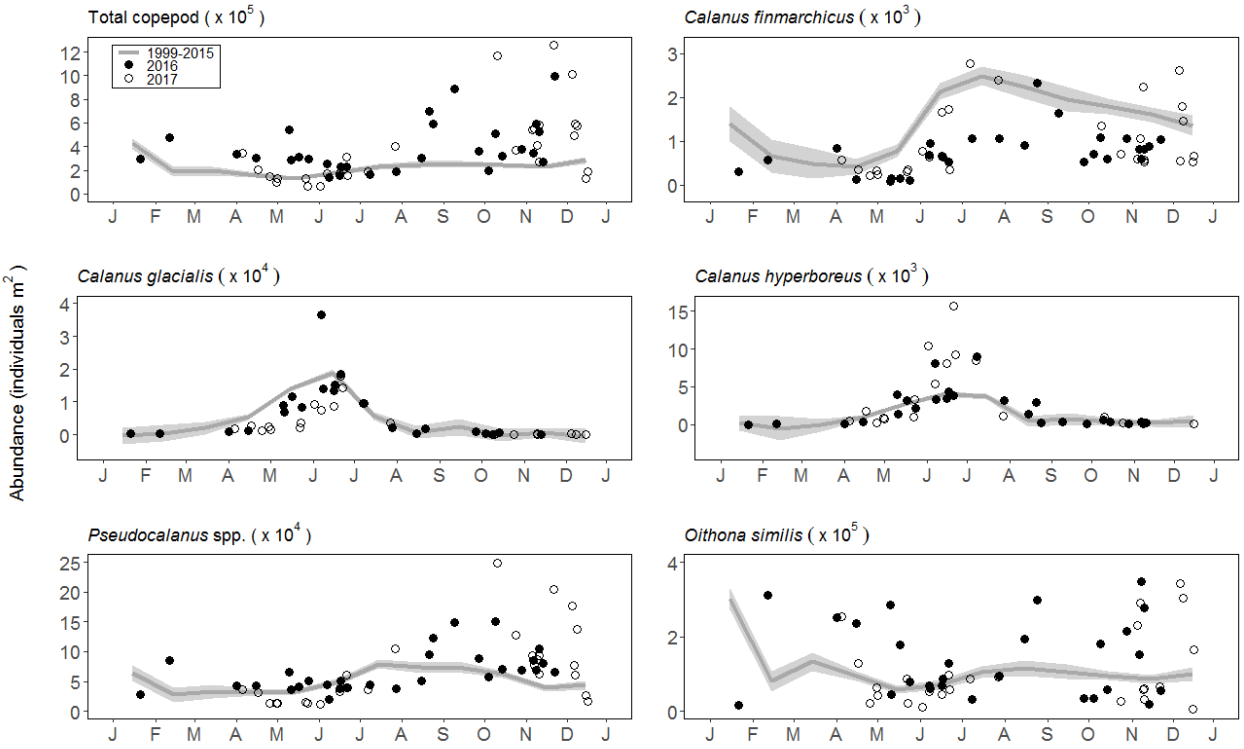

Figure 16. *Total copepod abundance (upper left panel) and abundance of large Calanus finmarchicus (upper right panel), Calanus glacialis (center left panel), Calanus hyperboreus (center right panel) and small Pseudocalanus spp.(lower left panel), Oithona spp. (lower right panel) copepods at the high frequency sampling station S27 for the 1999-2015 reference period (grey line) and for 2016 (black circle) and 2017 (white circle). Monthly means (SE) for the reference period were calculated using least square means derived from a linear model with the factors Year (1999 to 2015), and Season (spring, summer and fall).*

Copepod phenology

Climatological seasonal cycle of *C. finmarchicus* copepodite stages I to VI (CI-CVI) at S27 indicates that the relative abundance of adults (CVI) typically increases from January to a peak at ~55% in April, rapidly declines during spring, and levels at ~5% from June to December. Stage I copepodites (CI) peaks in May at ~55% and gradually decrease until September as individuals successively develop into CII to CV stages. From September to December, abundance is dominated by CV stages until copepodites start developing into adults in January (Figure 19). In 2016 and 2017, abundance of adults (CVI) peaked one month later (May) than climatology delaying the production cycle of the youngest copepodite stages. Stage I copepodites (CI) peaked in June in both years, and abundance of stage II and III (CII-CIII) remained high until September in 2016. In 2017, characterization of copepodite production cycle prior to adult (CVI) peak abundance and following emergence of stage I copepodites (CI) was limited by considerable sampling gaps during winter and late summer (Figure 17).

Climatological seasonal cycle of *Pseudocalanus* spp. copepodites stages also indicates that the relative abundance of adults (CVI) increases from January to a maximum of ~ 50% in April, before declining during spring and leveling at ~12% from June to December. The abundance of stage I copepodites (CI) also peaks in May at a lesser proportion (~16%) than that of *C. finmarchicus*, and gradually declines until September as individuals successively develop into the later stages. From September to January, CIV and CV remain the most abundant

copepodite stages, each at ~30% of total abundance. The peak abundance of adults recorded in April 2016 and 2017 lines up with climatology although the absence of data for the previous month(s) did not permit to determine if these represented annual maximums. Stage I copepodites (CI) peak abundance occurred one month later than climatology in both years. The development cycle of copepodite stages was also delayed in 2016 with 9% more CIII, 3% less CIV, and 7% less CV in November compared to climatology. In 2017, the structure of copepodite production cycle in autumn (October – December) was similar to climatology (Figure 17).

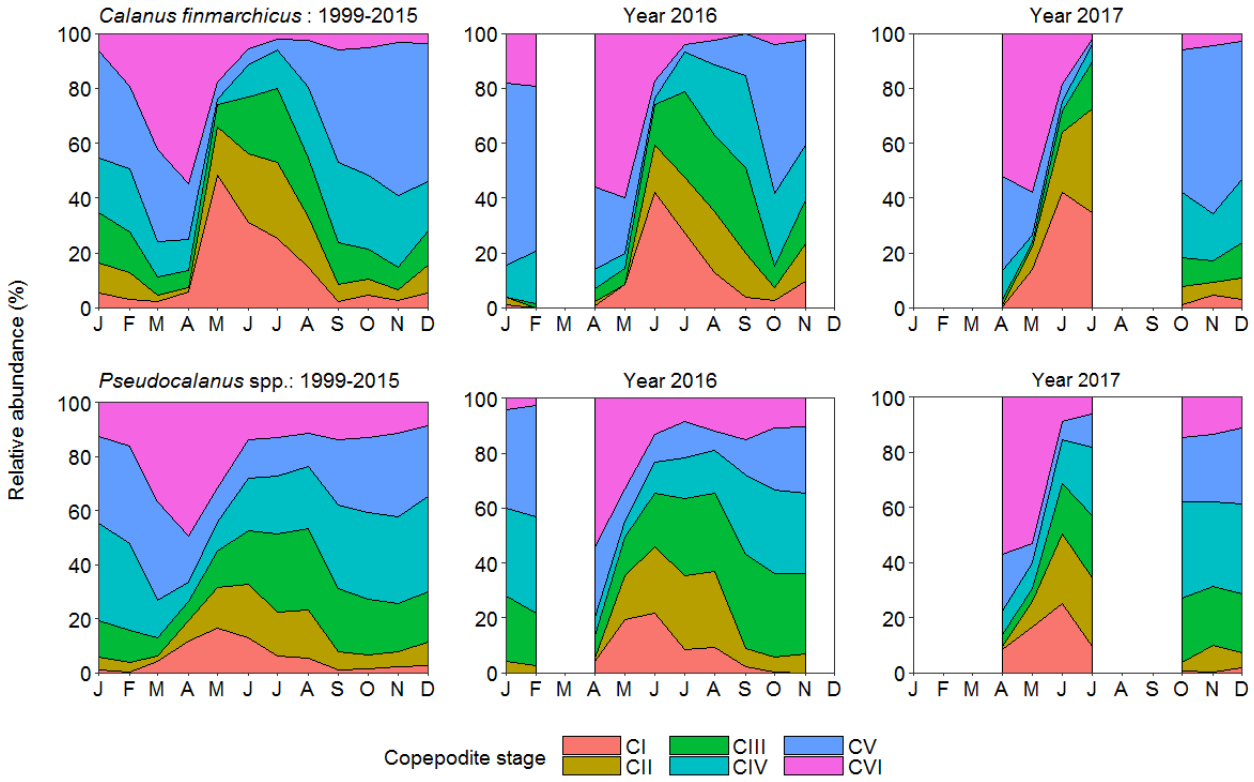

Figure 17. *Intra-annual variation in the relative abundance of copepodite stage I-VI for Calanus finmarchicus (top panels) and Pseudocalanus spp. (bottom panels) for the 1999-2015 reference period, and during the sample years 2016 and 2017. White rectangles in the middle (year 2016) and right (year 2017) panels represent period of the year with no data collection.*

Oceanographic sections

Zooplankton biomass

Zooplankton biomass showed similar trends on the Grand Banks (Southeast Grand Bank (SEGB), Flemish Cap (FC)) and the northeastern Newfoundland and southern Labrador Shelves over the past 19 years. Biomass was mostly below normal from 1999-2001, near or above normal from 2002-2011, and back to below normal from 2012-2017. In 2016 and 2017, zooplankton biomass remained low across all sections including time series record low on the SEGB section in 2016, and on the FC and Seal Island (SI) sections in 2017 (Figure 18).

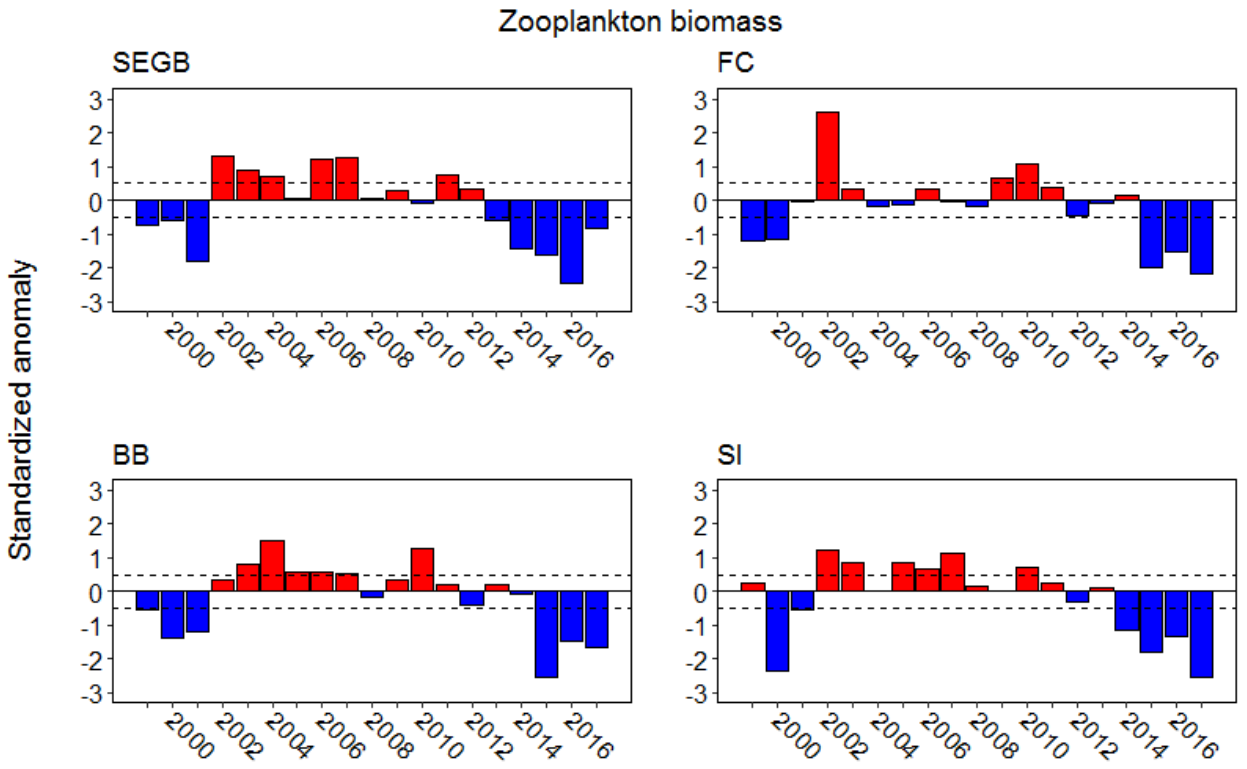

Figure 18. *Annual standardized anomalies of zooplankton biomass on four oceanographic sections [Southeast Grand Bank (SEGB); Flemish Cap (FC); Bonavista Bay (BB); Seal Island (SI)], from 1999 to 2017. Annual anomalies of log transformed biomass [ln (biomass g m^{-2} + 1)] were calculated for each section using least square mean (ls mean) and standard deviation (SD) derived from a linear model with fixed factors Year, Season and Station. Mean log transformed biomass (SD) for the 1999-2015 the reference period were: SEGB = 2.96 (0.93); FC = 4.88 (1.04); BB = 6.97 (2.31); SI = 6.27 (2.63). Anomalies within ±0.5 SD (horizontal dashed lines) of the reference period mean are considered normal.*

Zooplankton abundance

Since the beginning of the AZMP in 1999, zooplankton abundance has shown clear overall increasing trends over all sections. Anomalies transitioned from being mostly negative from 1999-2007 with the exception of positive anomalies from 2004-2006 for the SI section, to mostly positive from 2008 to 2017. Abundance anomalies for 2016 and 2017 were respectively the second highest and highest of the 19-y time series across all sections (Figure 19).

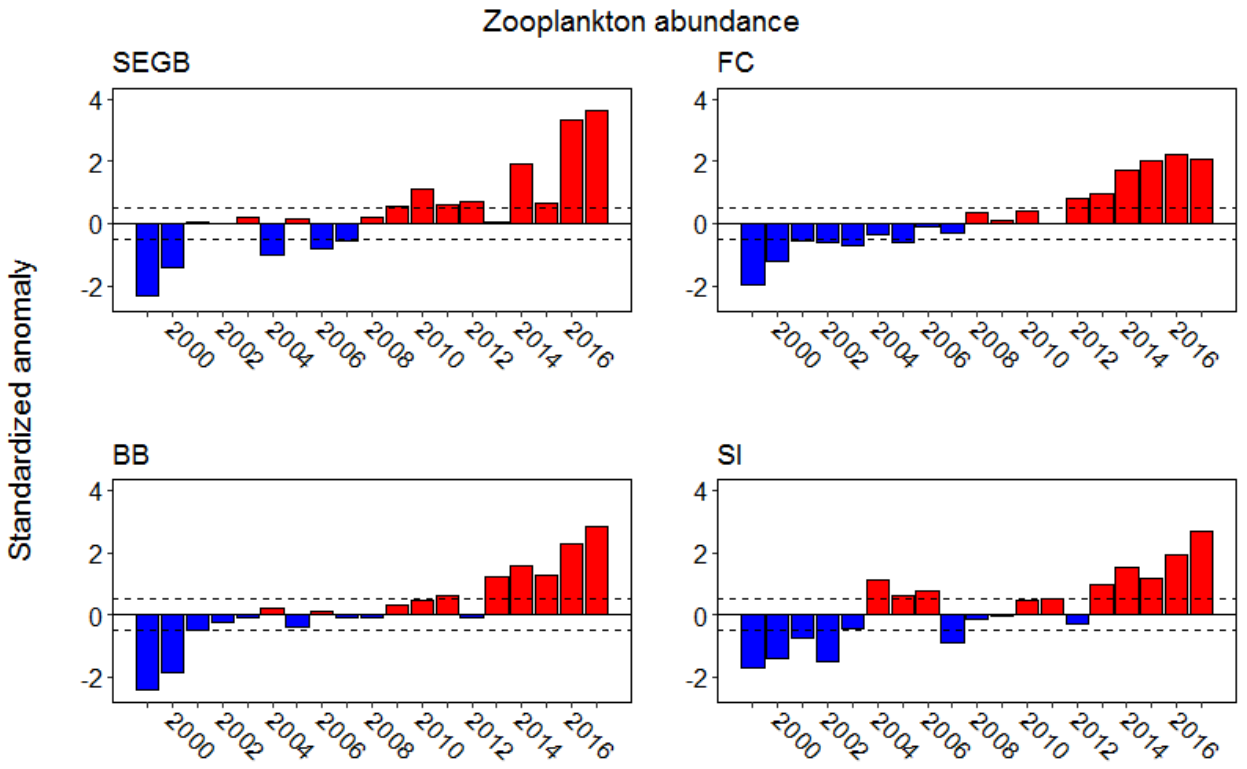

Figure 19. *Annual standardized anomalies of zooplankton abundance on four oceanographic sections [Southeast Grand Bank (SEGB); Flemish Cap (FC); Bonavista Bay (BB); Seal Island (SI)] from 1999 to 2017. For each section, annual anomalies of log transformed abundance [ln (individuals m^{-2} + 1)] were calculated using least square means derived from a linear model with fixed factors Year, Season and Station. Mean log transformed abundances (SD) for the 1999-2015 reference period were: SEGB = 118.36 (10.50); FC = 121.88 (13.48); BB = 135.01 (12.10); SI = 116.65 (15.18). Anomalies within ±0.5 SD (horizontal dashed lines) of the reference period mean are considered normal.*

Calanus finmarchicus

There is no clear trend for abundance of the large calanoid copepod *C. finmarchicus* on the Grand Banks (SEGB and FC) with negative and positive anomalies alternating every 1-5 y since 1999. Abundance on the SEGB section was back to above normal in 2017 with the second highest anomalies of the time series whereas anomalies on the FC section were positive in 2016 and 2017 after three consecutive years of negative anomalies. Abundance on the northeastern Newfoundland Shelf (BB) generally increased during the first eight years of the AZMP from a historical low in 1999 to record high in 2006. Abundance remained near or above normal until 2014 before dropping below the climatology and has remained at low levels through 2017. On the southern Labrador Shelf (SI), *C. finmarchicus* abundance also rapidly increased from a record low at the beginning of the time series in 2000, to a record high in 2004, before declining back to below normal in 2009. Abundance has since been alternating between positive and negative anomalies every 1-2 years. Abundance has remained mostly below normal since 2014 on the northeast Newfoundland and southern Labrador Shelves (BB and SI). The positive anomaly recorded at SI in 2016 was followed, in 2017, by the second lowest anomaly of the time series (Figure 20).

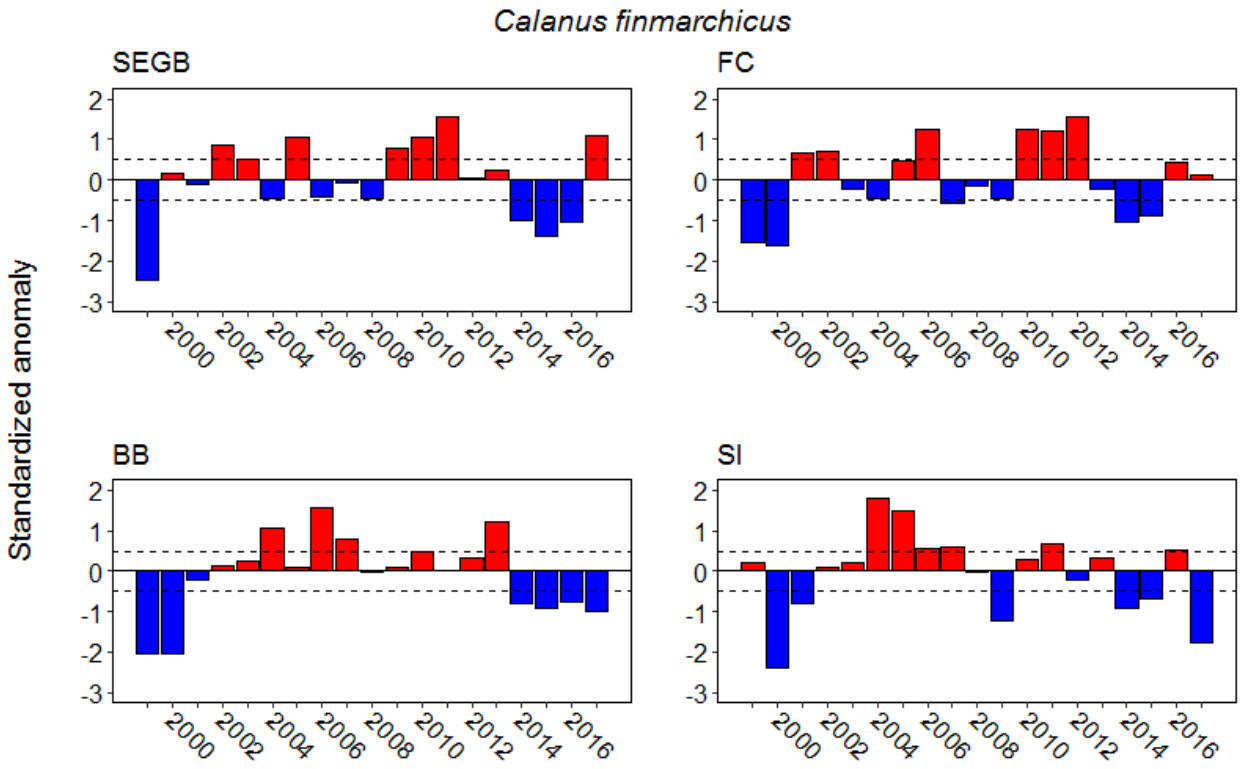

Figure 20. *Annual standardized anomalies of Calanus finmarchicus abundance on four oceanographic sections [Southeast Grand Bank (SEGB); Flemish Cap (FC); Bonavista Bay (BB); Seal Island (SI)] from 1999 to 2017. Annual anomalies of log transformed abundance [ln (individuals m^{-2} + 1)] were calculated using least square means derived from a linear model with fixed factors Year, Season and Station. Mean log transformed abundances (SD) for the 1999-2015 reference period were: SEGB = 8.04 (0.64); FC = 9.10 (0.34); BB = 9.66 (0.30); SI = 9.54 (0.68). Anomalies within ±0.5 SD (horizontal dashed lines) of the reference period mean are considered normal.*

Pseudocalanus spp.

The abundance of the small calanoid copepod *Pseudocalanus* spp. has been generally increasing on the Grand Banks (SEGB and FC) since 1999 with abundance consistently above normal since 2009 except for one year (2011) on the FC section. In 2016 and 2017, the abundance of *Pseudocalanus* spp. remained high on the Grand Banks with the two highest anomalies of the time series on the SEGB section and the second and third highest anomalies on the FC section. On the northeast Newfoundland Shelf (BB) abundance was low during the early 2000s and has been oscillating above and below normal every 1-3 y since 2003. On the southern Labrador Shelf (SI), abundance steadily increased from a record low in 1999 to a record high in 2004 before declining over the next 4 years. Abundance remained near or below normal from 2008 to 2014 but recently increased above normal for the first time in almost eight years. On the northeast Newfoundland Shelf (BB) abundance was back to near normal after three years of positive anomalies. On the southeastern Labrador Shelf, abundance was slightly above normal in 2016 and near climatology in 2017 (Figure 21).

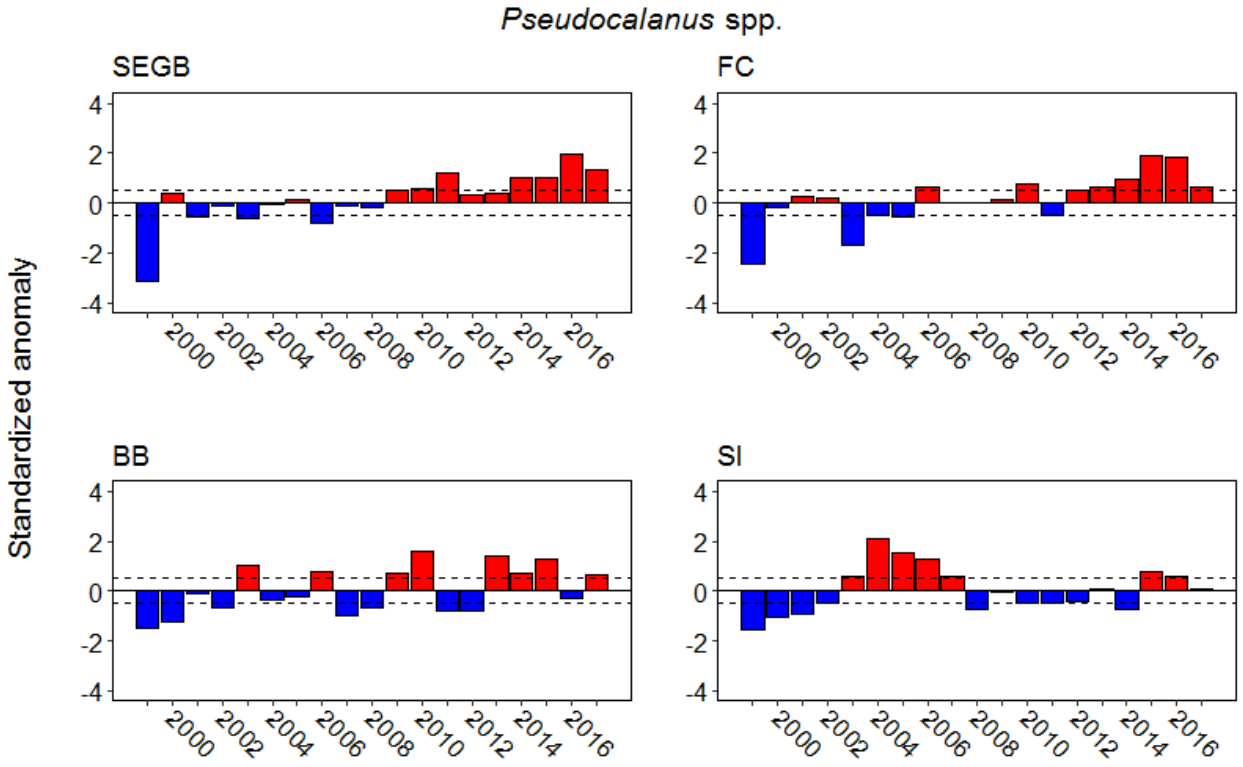

Figure 21. *Annual standardized anomalies of Pseudocalanus spp. abundance on four oceanographic sections [Southeast Grand Bank (SEGB); Flemish Cap (FC); Bonavista Bay (BB); Seal Island (SI)] from 1999 to 2017. Annual anomalies of log transformed abundance [ln (individuals m^{-2} + 1)] were calculated using least square means derived from a linear model with fixed factors Year, Season and Station. Mean log transformed abundances (SD) for the 1999-2015 reference period were: SEGB = 9.70 (0.42); FC = 8.42 (0.51); BB = 9.06 (0.39); SI = 9.92 (0.69). Anomalies within ±0.5 SD (horizontal dashed lines) of the reference period mean are considered normal.*

Oithona spp.

The abundance of *Oithona* spp., a complex of two small cyclopoid copepod species (*Oithona similis* and *Oithona atlantica*), that numerically dominates copepod assemblages in the Northwest Atlantic, has generally increased on the Grand Banks (SEGB and FC) and the northeast Newfoundland Shelf (BB) since the beginning of the monitoring program in 1999. *Oithona spp.* abundance remained above normal on the Grand Banks in 2016-2017 with a record high on SEGB and the second and third highest anomalies of the time series on FC. Abundance has remained mostly above normal on BB over the past 15 y with the exception of 2012 and 2014, the two lowest anomalies of the time series. On the southern Labrador Shelf (SI), abundance increased from 1999 to 2006, but was back to below normal in 2008 and has generally remained near or below normal through 2017. Abundance increased from normal in 2016 to a record high in 2017 on the BB section, and decreased from slightly above to below normal in 2016 and 2017, respectively (Figure 22).

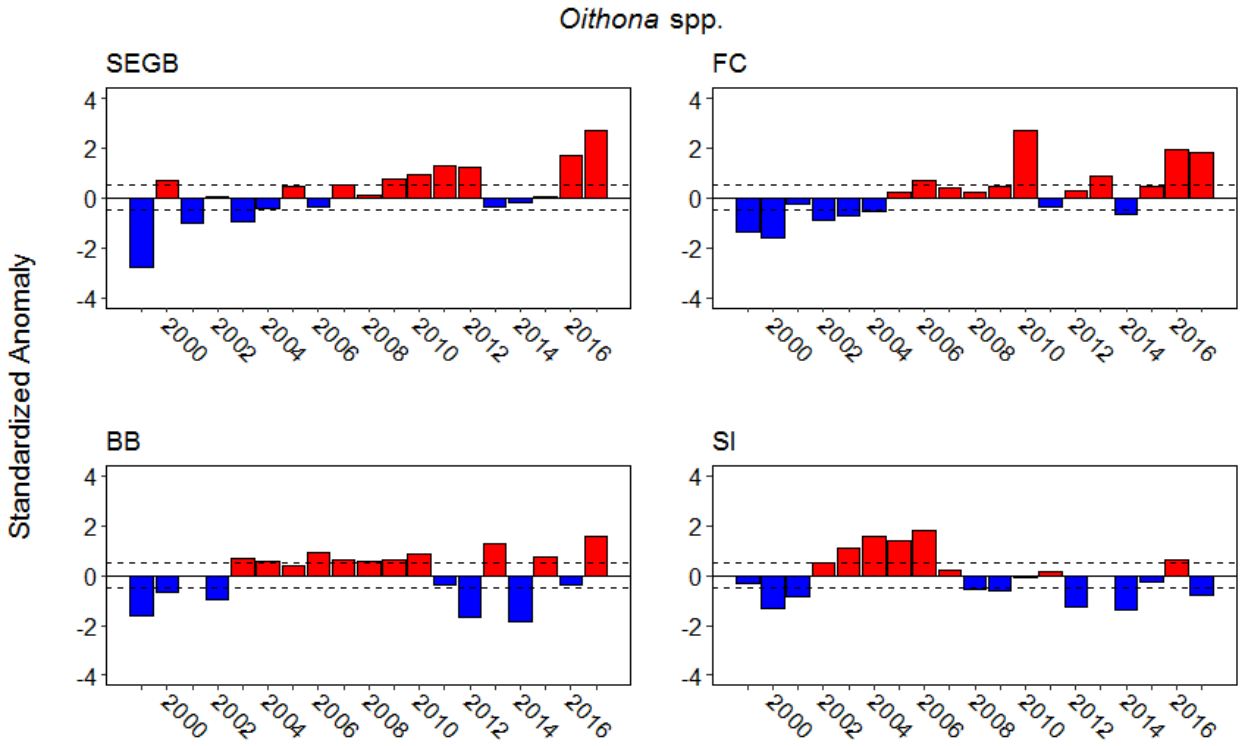

Figure 22. *Annual standardized anomalies of Oithona spp. abundance on four oceanographic sections [Southeast Grand Bank (SEGB); Flemish Cap (FC); Bonavista Bay (BB); Seal Island (SI)] from 1999 to 2017. Annual anomalies of log transformed abundance [ln (individuals m^{-2} + 1)] were calculated using least square means derived from a linear model with fixed factors Year, Season and Station. Mean log transformed abundances (SD) for the 1999-2015 reference period were: SEGB = 10.74 (0.31); FC = 10.43 (0.31); BB = 10.25 (0.30); SI = 10.24 (0.77). Anomalies within ±0.5 SD (horizontal dashed lines) of the reference period mean are considered normal.*

Non-copepod zooplankton

The abundance of non-copepod zooplankton taxa has recently increased by several orders of magnitude across the region compared to the reference period. Time-series highs were attained in 2016 and 2017 for all sections with anomalies ranging between 2.1 and 3.4 SD above the climatology. Non-copepod abundance on the SEGB fluctuated between above and near normal since 2013 whereas other sections to the north (FC, BB and SI) exhibited a clear increasing trend during the same period with five consecutive years of positive anomalies (Figure 23).

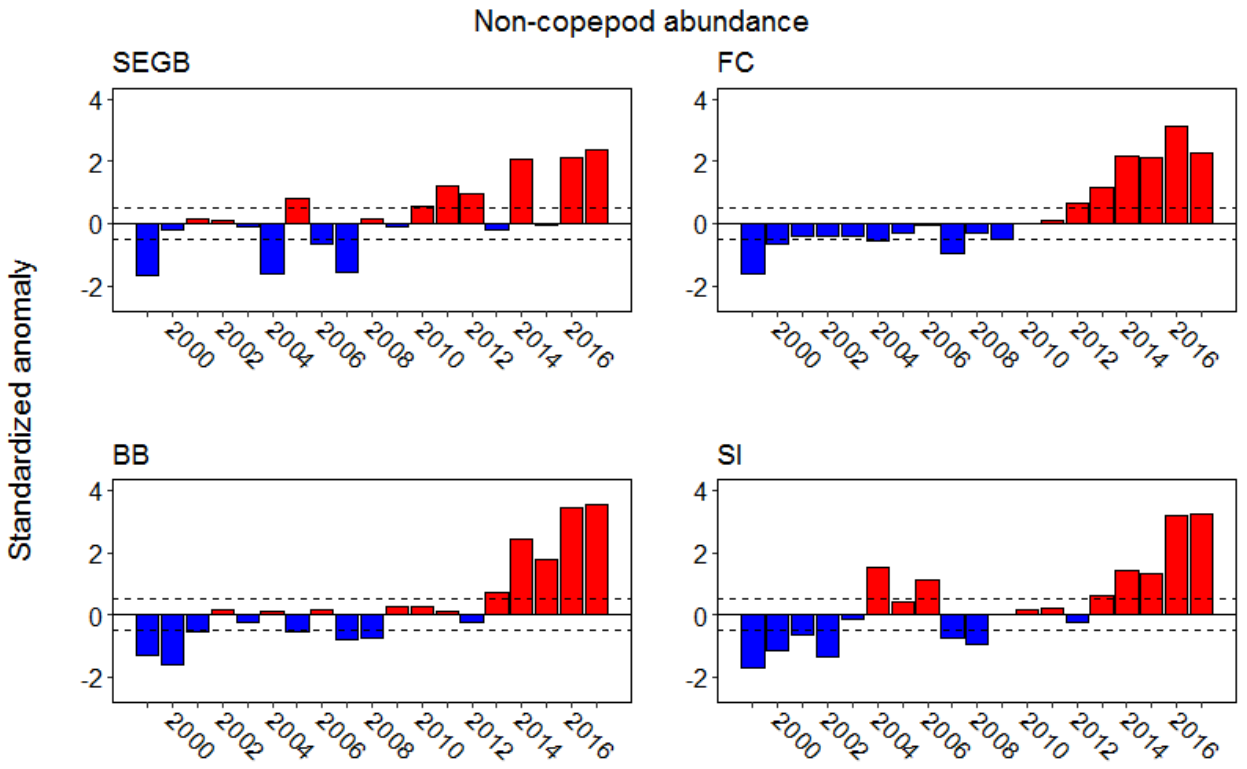

Figure 23. *Annual standardized anomalies of non-copepod abundance on four oceanographic sections [Southeast Grand Bank (SEGB); Flemish Cap (FC); Bonavista Bay (BB); Seal Island (SI)] from 1999 to 2017. Annual anomalies of log transformed abundance [ln (individuals m^{-2} + 1)] were calculated using least square means derived from a linear model with fixed factors Year, Season and Station. Mean log transformed abundances (SD) for the 1999-2015 reference period were: SEGB = 35.53 (4.18); FC = 33.54 (6.02); BB = 34.11 (4.77); SI= 31.21 (6.51). Anomalies within ±0.5 SD (horizontal dashed lines) of the reference period mean are considered normal.*

Non-copepod zooplankton assemblages along the different sections are dominated by tunicates (mainly *Oikopleura* spp. and *Fritilla borealis*) and by planktonic mollusks such as the pelagic gastropod *Limacina* spp. Together, these two taxa account for 56% to 92% of the non-copepod abundance. On the SEGB section, the relative proportion of tunicates decreased from a record high of 79% in 2013 to respectively 39% and 30% in 2016 and 2017, the latter being the lowest values in 15 years. The abundance of planktonic mollusk approximately doubled during the same period, and their proportion increased from 10% to 44%. On the FC section the proportion of tunicates markedly increased from a record low in 2010 of 25%, to a record high in 2016 (73%) before declining to 37% in 2017. Here again, the decrease in tunicate relative abundance between 2016 and 2017 was associated with a 23% increase in mollusk proportion. On the BB section, the proportion of tunicates generally increases from 2010 to a record high of 49% in 2017. On the SI section, tunicate relative abundance markedly increased from 24% in 2015 (second lowest value of the time series) to respectively 61% and 75% in 2016 and 2017, the latter being the highest recorded value in ten years. The proportion of mollusks in 2016 and 2017 dropped below 20% for the first time of the time series on the BB section, and below 10% for the first time since 2002 on the SI section. Abundance of non-copepod crustaceans was largely dominated by ostracods, euphausiids and cladocerans on the Grand Banks (SEGB and FC), and by ostracods and euphausiids on the northeast Newfoundland (BB) and southern Labrador (SI) Shelves. Mean relative abundance of non-copepod crustaceans varied between

10% (SEGB) and 22% (BB) and did not show clear temporal trends on any of the oceanographic sections (Figure 24).

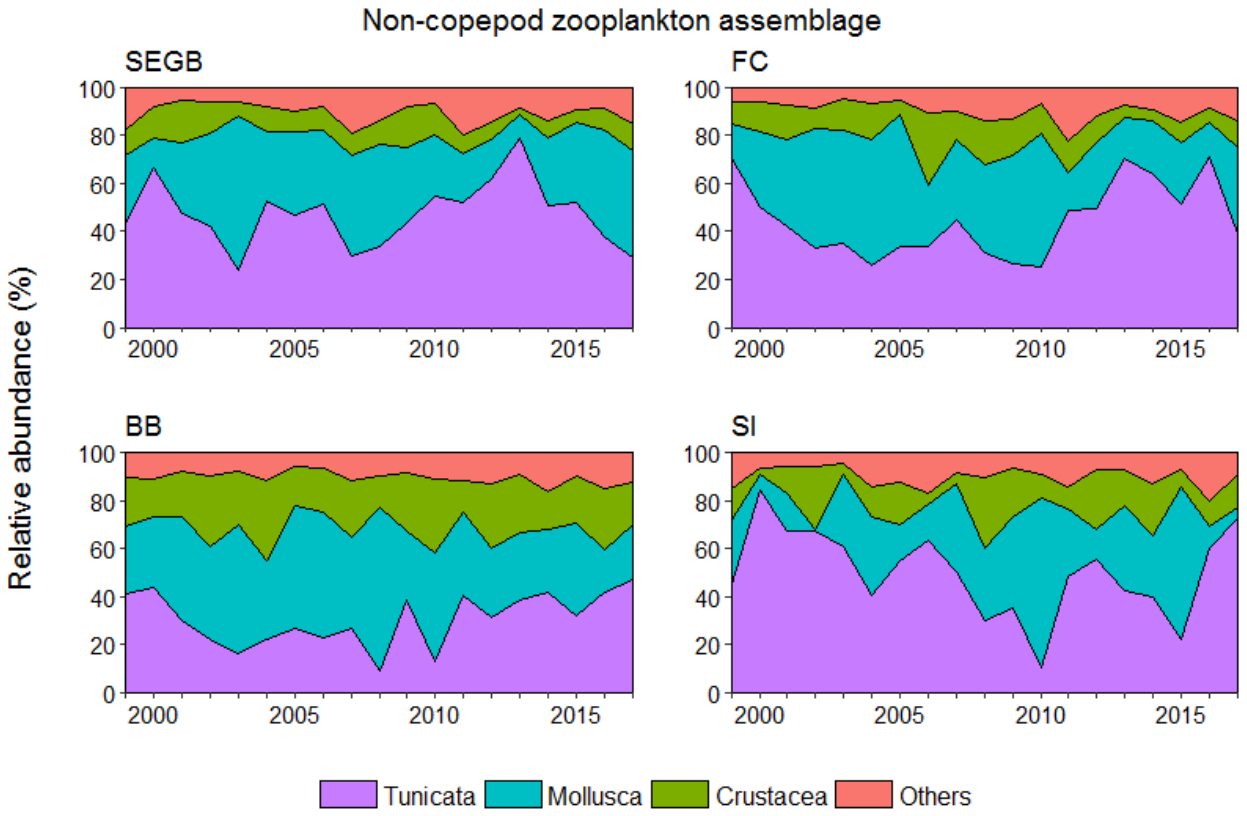

Figure 24. *Annual relative abundance of main non-copepod zooplankton groups on four oceanographic sections [Southeast Grand Bank (SEGB); Flemish Cap (FC); Bonavista Bay (BB) Seal Island (SI)] from 1999 to 2017.*

Spatial distribution

In the spring of 2016 and 2017, the highest abundances of zooplankton were encountered in the Avalon Channel, the Flemish Pass and on the SEGB shelf break (Figure 25). In summer, zooplankton highest abundances occurred over the Flemish Cap and in outer shelf break waters of the BB (2017 only) and FC sections. Zooplankton distribution patterns along the BB and FC sections were similar for both years but abundance decreased on the SI section in 2017 compared to 2016 (Figure 26). In autumn 2016, zooplankton was present in high concentration in the Avalon Channel and in the shallow waters (<100 m) of the southeastern Grand Banks. In 2017, the highest abundances were encountered on the shelf break of the BB section and on the eastern half of the Grand Banks along the FC section (Figure 27).

In general, sampling stations with high zooplankton concentration were spatially aggregated in areas associated with boundary currents like the oceanic front between the Labrador current and Gulf Stream on the tail of the Grand Banks and the Flemish Cap area, and/or with topographic features such as the Avalon Channel, the Flemish Cap/Pass and the shelf break. Overall abundances in 2016 and 2017 were higher than the climatology in all oceanographic sections except for BB in summer 2016, and SI in summer 2017, where abundance patterns were similar to climatology. Comparison of zooplankton distribution pattern between 2016 and 2017 is limited by the absence of shared oceanographic sections during autumn surveys for these two years (Figure 25, 26 & 27).

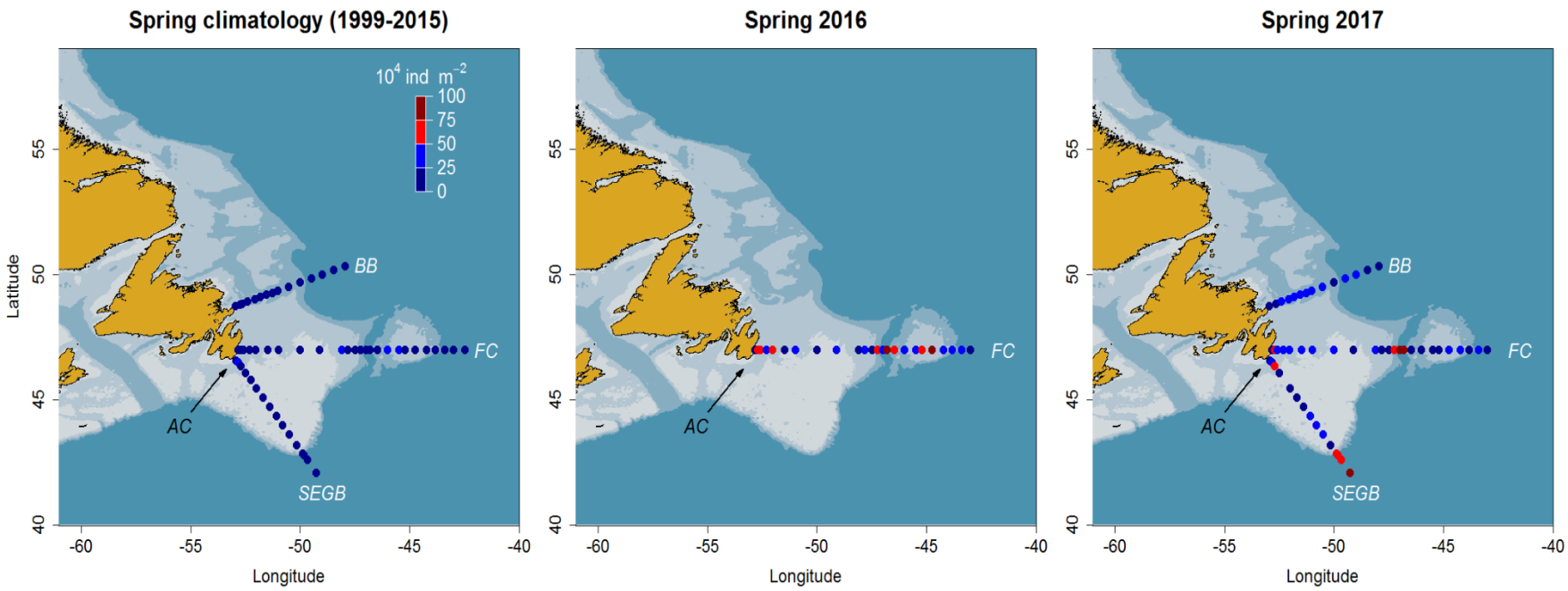

Figure 25. *Spring zooplankton abundance per station along three oceanographic sections [Bonavista Bay (BB); Flemish Cap (FC); Southeast Grand Bank (SEGB)] for the climatological reference period (left), year 2016 (middle) and 2017 (right). Lighter to darker colour gradient of the ocean represents the 100, 300 and 1000 m isobaths. Black arrow indicates the location of the Avalon Channel (AC).*

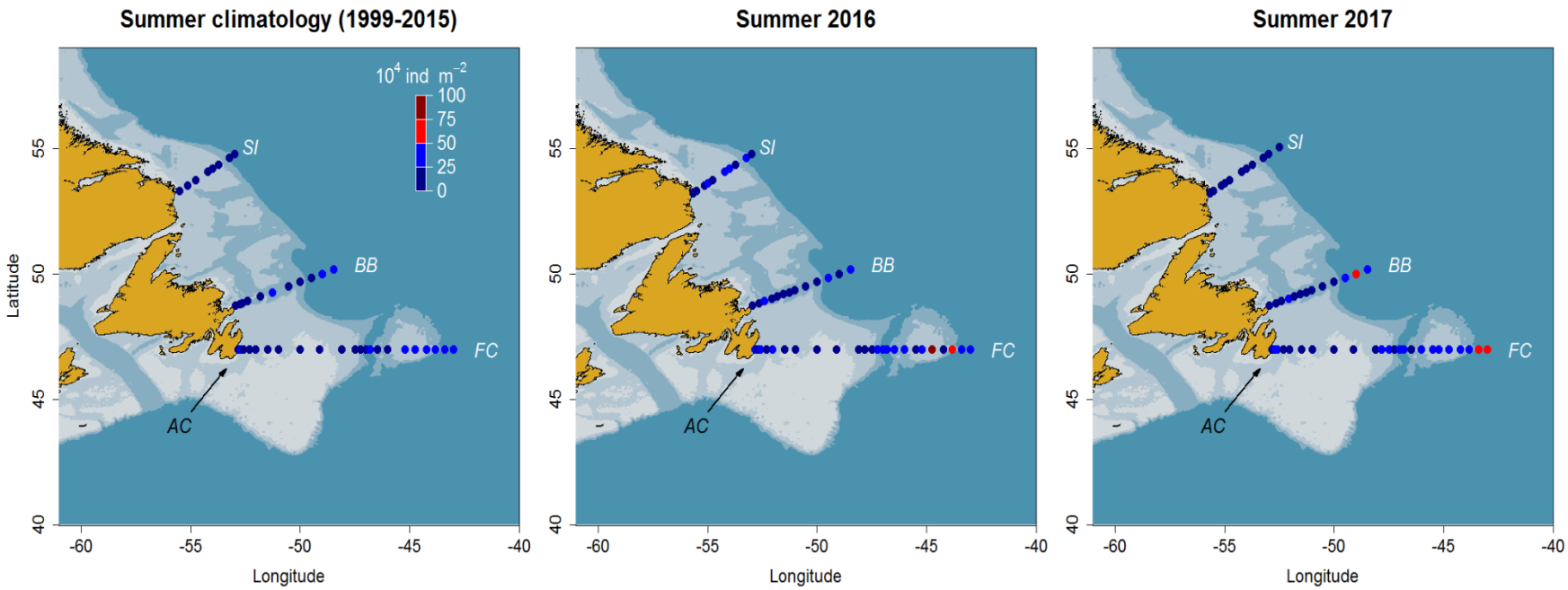

Figure 26. *Summer zooplankton abundance per station along three oceanographic sections [Seal Island (SI); Bonavista Bay (BB); Flemish Cap (FC)] for the climatological reference period (left), year 2016 (middle) and 2017 (right). Lighter to darker colour gradient of the ocean represents the 100, 300 and 1000 m isobaths. Black arrow indicate the location of the Avalon Channel (AC).*

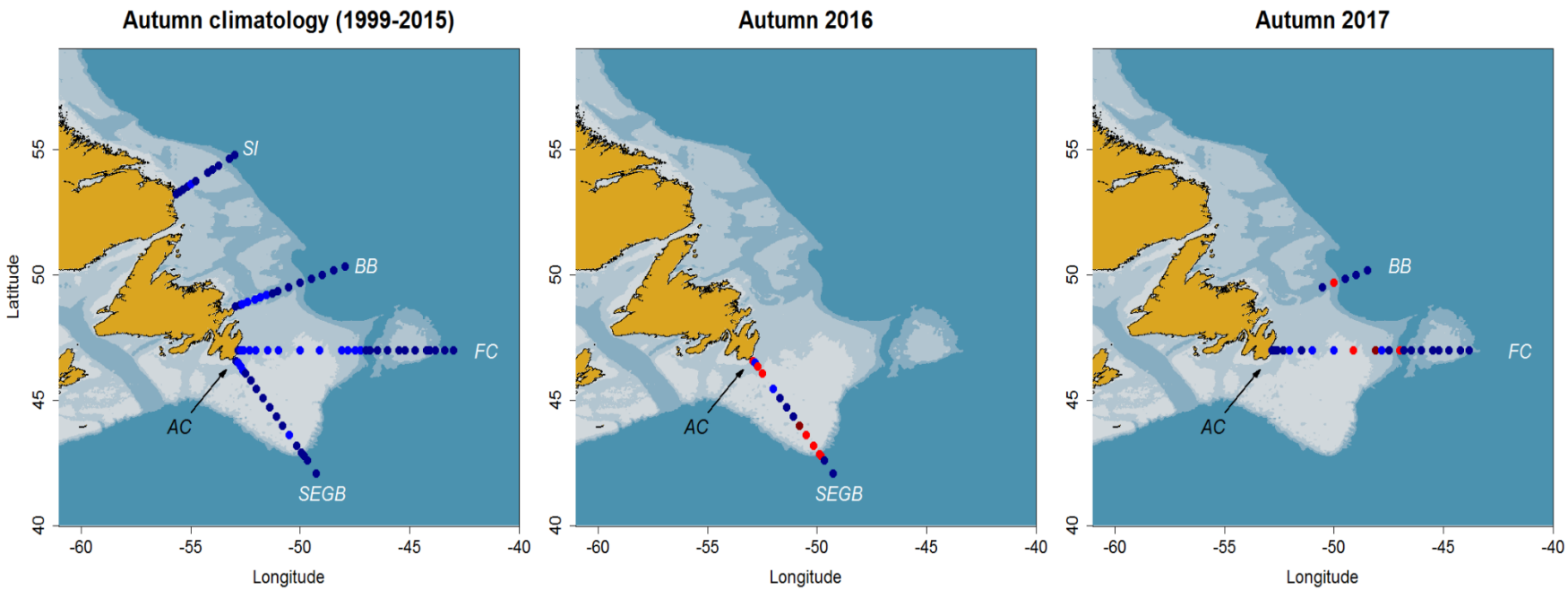

Figure 27. *Autumn zooplankton abundance per station along four oceanographic sections [Seal Island (SI); Bonavista Bay (BB); Flemish Cap (FC); Southeast Grand Bank (SEGB)] for the climatological reference period (left), year 2016 (middle) and 2017 (right). Lighter to darker colour gradient of the ocean represents the 100, 300 and 1000 m isobaths. Black arrow indicate the location of the Avalon Channel (AC).*

DISCUSSION

Observations of phytoplankton biomass inferred from optical and pigment indices at the high frequency sampling station (S27) indicate reduction in the spring bloom in recent years compared to long-term observations. Lower productivity can also be associated with higher mortality through impacts of grazing by zooplankton. The physical habitat indices at S27 have gradually shifted back to normal after a period of general cooling and freshening of water masses along with associated changes in larger sea ice extent and higher stratification (Cyr et *al.* 2018). Cooling and freshening may influence phytoplankton by limiting the availability of solar radiation due to the presence of sea ice, reduced wind mixing of deep macronutrients into the euphotic zone due to enhanced stratification, and reduced growth rates due to colder temperatures. The large reduction in observed phytoplankton biomass at S27 may be related to the above physical processes but the increase in the abundance of small copepods observed in recent years may also contribute to higher grazing pressure on standing stocks. The observed drawdown of macronutrients at S27 in recent years appears to be consistent with the long-term climatology, indicating higher predation pressure may be the principle cause of reduced standing stock of phytoplankton although reduced sampling occupations in 2016-2017 may have also resulted in missing a portion of the spring bloom signal. Large-scale synoptic coverage of near-surface ocean colour indices over the Newfoundland and Labrador Shelf indicate ongoing declines in phytoplankton biomass during the spring bloom. The record low inventories of macronutrients observed during 2010-2013 in both shallow and deep layers across the standard oceanographic sections, which may be associated with lower primary production, have since recovered to near normal levels in 2016-2017. The shift to later timing of the spring bloom observed at S27 in recent years is also consistent with the large-scale ocean colour imagery over the NL Shelf indicating the influence of large-scale environmental forcing.

The large-scale dominant pattern of increasing zooplankton abundance observed in NL shelf waters since the beginning of the AZMP in 1999 has continued through 2017. On the Grand Banks and the northeast Newfoundland Shelf, increased zooplankton abundance seems to be driven mainly by the abundance of the small copepod species *Pseudocalanus* and *Oithona* taxa. On the southern Labrador Shelf the abundance of these taxa has remained close to normal since 2007 and therefore cannot explain the increasing trend observed on the SI section. Other small copepod taxa such as *Oncaea* and *Microcalanus* spp. along with gelatinous zooplankton (e.g. Appendicularia) have increased by factors of ~1.5 and 2, respectively, compared to the climatology. However, the contribution of small copepods to the overall zooplankton biomass is limited, as shown by the important decline in biomass concurrent with record high abundances over the past 3-4 years. Zooplankton biomass on the Grand Banks and NL Shelves is normally seasonally dominated by large, energy-rich copepods that are critical to energy transfer to higher trophic levels, including planktivorous stages of several ecologically and economically important fish species. *Calanus finmarchicus* is the most abundant and widely distributed of the large calanoid copepods and the main contributor to mesozooplankton biomass in the Northwest Atlantic. Similarities between anomaly variation patterns of *C. finmarchicus* abundance and zooplankton biomass confirm the strong link between the abundance of large calanoid copepods and total zooplankton biomass in the system. Abundance trends from S27 and the SEGB and FC sections suggest a recent recovery of *C. finmarchicus* on the Grand Banks. The important increase in *C. finmarchicus* observed in 2017 on the SEGB section was associated with an increase of biomass from a record low in 2016 to a near normal level the following year. However, since 2015, biomass has remained at its lowest along the FC section despite a shift in abundance from below to above normal during the same period. Interestingly, the biomass of small zooplankton (<1 mm) at S27 also remained below normal in 2016 and 2017 despite the high abundance of small copepods, which normally

dominate the small size fraction along with the early life stages of calanoid copepods. A higher proportion of small soft-bodied larvaceans combined with a decrease in the relative abundance of calcifying taxa (Mollusca) may have overridden the effect of increased copepod abundance on zooplankton dry biomass in some areas of the shelf. The recent increases in the abundance of non-copepod zooplankton significantly contributed to the overall increase in zooplankton abundance observed across the study region. However, no specific taxonomic group emerged as solely responsible for this increase in non-copepod abundance.

Timing is a key mechanism affecting trophic interactions in variable environments, and temporal mismatch between trophic levels can have profound cascading effects on ecosystem community structure. The delayed onset of the spring bloom observed since 2012, coupled with general cooling and freshening (Cyr et al. 2018), may be partly responsible for the delay in the production cycle of *C. finmarchicus* adult (CVI) and youngest copepodite stages (CI) at S27 in 2016 and 2017 as well as for the general taxa. Recorded peak abundance of adults *Pseudocalanus* spp. in 2016 and 2017 was coincident with climatology, although gaps in sampling obscured the timing of production of CVI stages. Production of CI was also delayed ~1 month for *Pseudocalanus* spp. in 2017 but the sampling interruption from July to October limits our interpretation of the effect of a delayed copepodite seasonal cycle on the population phenological structure at a time of the year when abundance is normally highest.

The overall pattern of variation among nutrients, phytoplankton biomass and zooplankton abundance highlights the relationship between biogeochemical conditions (nitrate standing stock) and primary (phytoplankton biomass) and secondary (zooplankton biomass) production. There are persistent signs indicating a shift in copepod community structure characterized by a general decline of large energy-rich calanoid copepods in favor of smaller calanoid and cyclopoid species. More research is needed to understand the reasons behind these important changes in zooplankton community structure and their potential impact on the system at higher trophic levels.

SUMMARY

- In general, the optical indices and chlorophyll inventories associated with the spring bloom were generally below the climatology in 2016-2017.
- The shallow (< 50m) and deep (> 50m) macronutrient inventories along the standard ocean sections returned to near normal levels in 2016-2017.
- The chlorophyll *a* inventories inferred from the seasonal NL oceanographic surveys and fixed station remain below normal in 2016-2017 but have gradually increased since the record low observed in 2015.
- The metrics of the spring bloom derived from satellite imagery indicate the magnitude and amplitude of the spring production cycle were below normal across most of the NL sub-regions in 2016 (record-low) and 2017 compared to the climatology.
- Spring blooms started later than normal in 2016 and 2017, but duration was longer than normal based on satellite imagery.
- Zooplankton abundance continued to increase in 2016 and 2017 on the Grand Banks, the northeast Newfoundland Shelf, and southern Labrador Shelf. Abundance on each of the main oceanographic sections in 2016 and 2017 represented the second highest and highest anomalies since the beginning of the AZMP in 1999.

- Zooplankton biomass remained below normal in 2016 and 2017 on the Grand Banks and the northeastern Newfoundland and southern Labrador Shelves. New time series record low values were recorded in 2016 or 2017 on three of the four main oceanographic sections.
- The abundance of the large calanoid copepod *Calanus finmarchicus* increased on the Grand Banks, and anomalies were back to above normal in 2016 and 2017 on the FC and SEGB sections, respectively. Abundance remained generally below normal on the northeastern Newfoundland and southern Labrador Shelves.
- The abundance of the small calanoid copepod *Pseudocalanus* spp. remained high on the Grand Banks in 2016 and 2017 with some of the highest anomalies recorded since 1999 but decreased to near normal values on the northeastern Newfoundland and Labrador Shelves.

ACKNOWLEDGMENTS

We thank the many scientists and technicians at the Northwest Atlantic Fisheries Centre for collecting and providing much of the data contained in this analysis. Carla Caverhill and Cathy Porter at the Bedford Institute of Oceanography provided access to ocean colour data. We also thank the captains and crews of the CCGS Teleost, CCGS Needler, and CCGS Hudson for oceanographic data collection during 2016 and 2017. We thank Catherine Johnson and Marjolaine Blais for reviewing the document.

REFERENCES

Blais, M., Devine, L., Lehoux, C., Galbraith, P.S., Michaud, S., Plourde, S., and M. Scarratt. 2018. Chemical and Biological Oceanographic Conditions in the Estuary and Gulf of St. Lawrence during 2016. DFO Can. Sci. Advis. Sec. Res. Doc. 2018/037. iv + 57 pp.

Cyr, F., Colbourne, E., Holden, J., Snook, S., Han, G., Chen, N., Bailey, W., Higdon, J., Lewis, S., Pye B. and D. Senciall. 2019. Physical Oceanographic Conditions on the Newfoundland and Labrador Shelf during 2017. DFO Can. Sci. Advis. Sec. Res. Doc. In press.

DFO. 2018. Oceanographic Conditions in the Atlantic Zone in 2017. DFO Can. Sci. Advis. Sec. Sci. Advis. Rep. 2018/039.

Johnson, C., Devred, E., Casault, B., Head, E., and Spry, J. 2018. Optical, Chemical, and Biological Oceanographic Conditions on the Scotian Shelf and in the Eastern Gulf of Maine in 2016. DFO Can. Sci. Advis. Sec. Res. Doc. 2018/017. v + 58 p.

Mitchell, M. R., Harrison, G., Pauley, K., Gagné, A., Maillet, G., and P. Strain. 2002. Atlantic Zonal Monitoring Program sampling protocol. Can. Tech. Rep. Hydrogr. Ocean Sci. 223: iv + 23 pp.

Platt, T., Sathyendranath, S., Caverhill, C.M., and M.R. Lewis. 1988. Ocean primary production and available light: further algorithms for remote sensing. Deep Sea Res. 35: 855 – 879.

Zhai, L., Platt, T., Tang, C., Sathyendranath, S., and R. Hernández Walls. 2011. Phytoplankton phenology on the Scotian Shelf. ICES J. Mar. Sci. 68(4): 781-791.